200
9/20/84 JS ②

DR-0415-4

DOE/FE/60177-1624
(DE84013369)

INVESTIGATION OF TRACER AND STEAM TESTS ON THE WESTERN RESEARCH INSTITUTE 150-TON RETORT

By
T. Fred Turner
Dennis F. Moore
Norman W. Merriam
James R. Covell

April 1984

Work Performed Under Contract No. FC21-83FE60177
For
U. S. Department of Energy
Office of Fossil Energy
Morgantown Energy Technology Center
Laramie, Wyoming
By
Western Research Institute
Laramie, Wyoming

Technical Information Center
Office of Scientific and Technical Information
United States Department of Energy

DISCLAIMER

DISCLAIMER

Available from the National Technical Information Service, U. S. Department of Commerce, Springfield, Virginia 22161.

Price: Printed Copy A04
Microfiche A01

Codes are used for pricing all publications. The code is determined by the number of pages in the publication. Information pertaining to the pricing codes can be found in the current issues of the following publications, which are generally available in most libraries: *Energy Research Abstracts (ERA); Government Reports Announcements* and Index (*GRA* and I); *Scientific and Technical Abstract Reports (STAR);* and publication NTIS-PR-360 available from NTIS at the above address.

DOE/FE/60177-1624
(DE84013369)
Distribution Category UC-91

INVESTIGATION OF TRACER AND STEAM TESTS ON THE WESTERN RESEARCH INSTITUTE 150-TON RETORT

By
T. Fred Turner
Dennis F. Moore
Norman W. Merriam
James R. Covell

April 1984

Work Performed Under Cooperative Agreement
DE-FC21-83FE60177

For
U. S. Department of Energy
Office of Fossil Energy
Morgantown Energy Technology Center
Laramie Project Office
Laramie, Wyoming

By
Western Research Institute
Laramie, Wyoming

TABLE OF CONTENTS

LIST OF FIGURES

List of Figures (cont.)

ABSTRACT

Gas tracer and steam front velocities in addition to flow model calculations are used to characterize rubble bed structure in an oil shale retort. The gas tracer method is shown to have superior resolution to the steam front method in detecting rubble bed variations. The tracer method is potentially less expensive. Recommendations for further research are made.

INTRODUCTION

Vertical modified in situ (VMIS) retorting of oil shale has been studied for several years as a potential source of hydrocarbons.[1,2,3] In this method a chimney of oil shale rubble is created by mining and blasting. The rubble is ignited at the top and airflow is established through the chimney. The burn front moves down through the retort heating the shale in front of it to retorting temperature. Oil mist produced, condenses farther down in the retort and flows to the collection system at the bottom. A typical rubble chimney is twenty to fifty meters on a side and one hundred to two hundred meters high. A retort in this size range contains fifty million to nine hundred million kilograms of oil shale and has a potential yield of four million to seventy million kilograms of shale oil.

One of the problems associated with the MIS process is the difficulty of forming a uniform rubble bed. A nonuniform rubble chimney causes poor distribution of airflow resulting in low sweep efficiency, which is defined as the fraction (by weight) of shale heated to retorting temperature by the retorting front. The overall product yield is related to sweep efficiency because channeling of the retorting front causes product to be burned, decreasing the yield.

To predict the flow behavior of a retort, one must first measure some of the properties of the rubble bed. Two rubble bed characterization methods with some history of success are steam front monitoring and gas tracer testing. The steam condensation front which precedes the retorting front has been found to map accurately the shape of that retorting front.[4] This method is used in two ways. First, the actual shape of the steam front can be determined if enough thermocouples are placed in the rubble. Second, a sweep efficiency can be calculated based on the total energy input into the retort before steam front break-through at the bottom of the retort. The other method, gas tracer testing, has been used on most of the larger MIS retorts.[1,2,3] This method requires that airflow be established through the retort followed by injection of a pulse of tracer gas into the retort at a predetermined location. The concentration of the tracer gas is monitored at detection points downstream from the injection point. Gas tracer measurements are repeated at different injection and detection points until the areas of interest in the rubble bed have been swept. The concentration data collected at the detection points can be used to calculate properties of the retort system such as gas velocities, dispersion constants, and void fractions.

The steam front monitoring method has two major weaknesses. First, the steam condensation front exists only after the retort has been ignited. There is little time for adjusting operating conditions to correct any flow nonuniformities discovered using steam front measurements. Running a separate steam test on a VMIS retort is prohibitively expensive. Second, unless thermocouples are placed throughout the rubble, there is no way of determining the locations of nonuniformities so that corrective procedures can be implemented.

The gas tracer method can be used prior to ignition and can indicate the general locations of nonuniformities. However, this method has several problems. First, the number of tracer tests that can be run is limited by economics and, in the case of radioactive tracers, by total allowed radioactive emissions while the number of flow channels in a retort is effectively infinite. This means that a complete description of a retort is impossible and that, depending on the number of tracer tests run and the regions through which this tracer passes, there is probably a minimum size of channel or obstruction that can be detected. The interpretation of tracer test results from MIS retorts has been limited because of these problems. The tracer testing method does, however, offer the greatest potential for improvement if some of its problems are defined and solved by appropriate research programs.

The current plan is to investigate the tracer testing method in nonuniform retorts and to define and address some of the problems with the method. This investigation includes a comparison of steam front measurements with tracer testing measurements and incorporates the use of flow models to aid in the interpretation of the tests. The largest available retort is used to minimize scale up problems. This report discusses some of the problems associated with tracer testing and shows how the steam front and model predictions compare with the tracer test results.

EXPERIMENT

The tests described have been run in Western Research Institute's (WRI) nominally sized, 150-ton, batch type, experimental oil shale retort located approximately one kilometer north of Laramie, Wyoming. The retort holds a rubble bed 3.505 meters in diameter and typically 13.11 meters in height. A more detailed description of the retort is found elsewhere.[5]

The retort is loaded with shale of a measured size distribution and is instrumented at four levels with eleven gas taps and thermocouples on each level as shown in figure 1. Probe level 1 is located approximately two meters from the top of the rubble bed and the other levels are spaced at 2.74 meter intervals down the retort. On each level a sampling tap and a thermocouple are placed at the centerline of the retort. Eight others are placed at 0.30 meter intervals to the north and south of the centerline. The last two taps and thermocouples on each level are located on the same line 1.68 meters from the centerline. Starting from the north side of the retort the taps on each level are designated A through K, where A and K are the taps near the walls and F is the tap on the centerline. The level number and the tap letter are used to describe each tap; for example, 1A means probe level 1 and tap A. A thermocouple and a gas sampling tap are also located at the outlet of the retort.

The tracer testing plan for the retort consists of two stages. In stage 1 the retort is tested after it is loaded to 1.4 meters above the

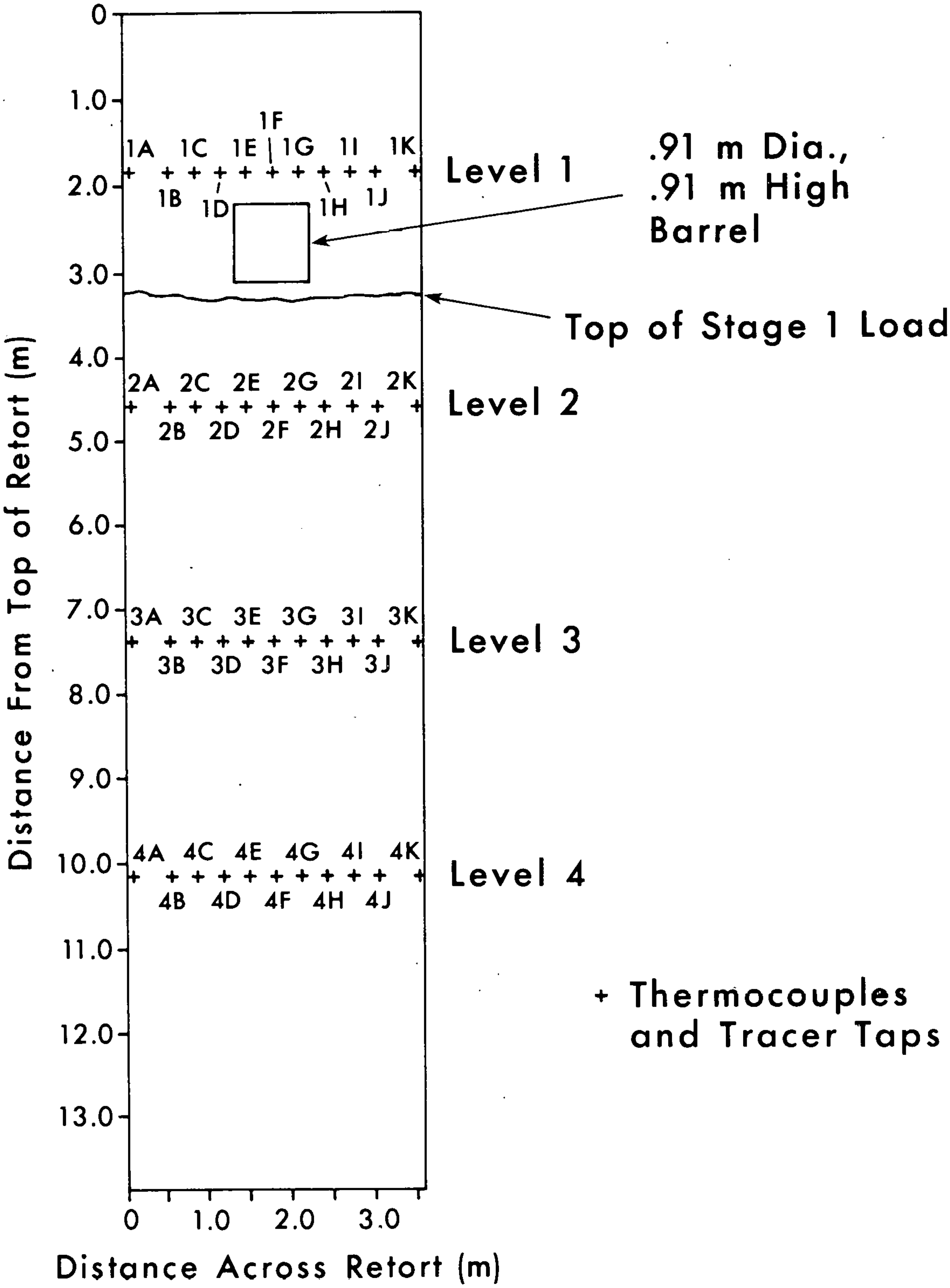

Figure 1. 150-Ton Retort Test Configuration

second probe level (see figure 1). This series of tests is designed to determine the properties of the unperturbed shale bed. After stage 1 the retort is opened and loading continues. At this time a cylindrical obstruction is placed on the center line of the retort. The obstruction is a 0.91 meter diameter, 0.91 meter high cardboard tube filled with oil shale and covered with a disc of plywood. The top of this obstruction is positioned 0.38 meters below probe level 1. Shale is added until the retort is filled to a level 0.81 meters below the top opening and 1.98 meters above probe level 1. After the retort is closed, the stage 2 tracer tests are begun.

The tracer testing system consists of a tracer injection system, a tracer detection system, and a tracer response analyzer. The injection system is shown schematically in figure 2. This system uses a fast, precision solenoid to release a timed pulse of tracer from a constant pressure reservoir. This pulse travels through the gas sampling tube into the retort. Accurate, reproducible injections are possible with this injection system. A typical injection consists of a two or three second wide pulse at a tracer reservoir pressure of 345 kPa. Krypton-85 (Kr-85), the radioactive tracer gas chosen for these tests, has been used extensively on both large and small oil shale retorts.(1)

The use of a radioactive tracer allows a relatively simple and expandable detection system to be used. This detection system is shown schematically in figure 3. The positive pressure on the retort provides sample gas flow through the sample tap tubes to the detection chambers.

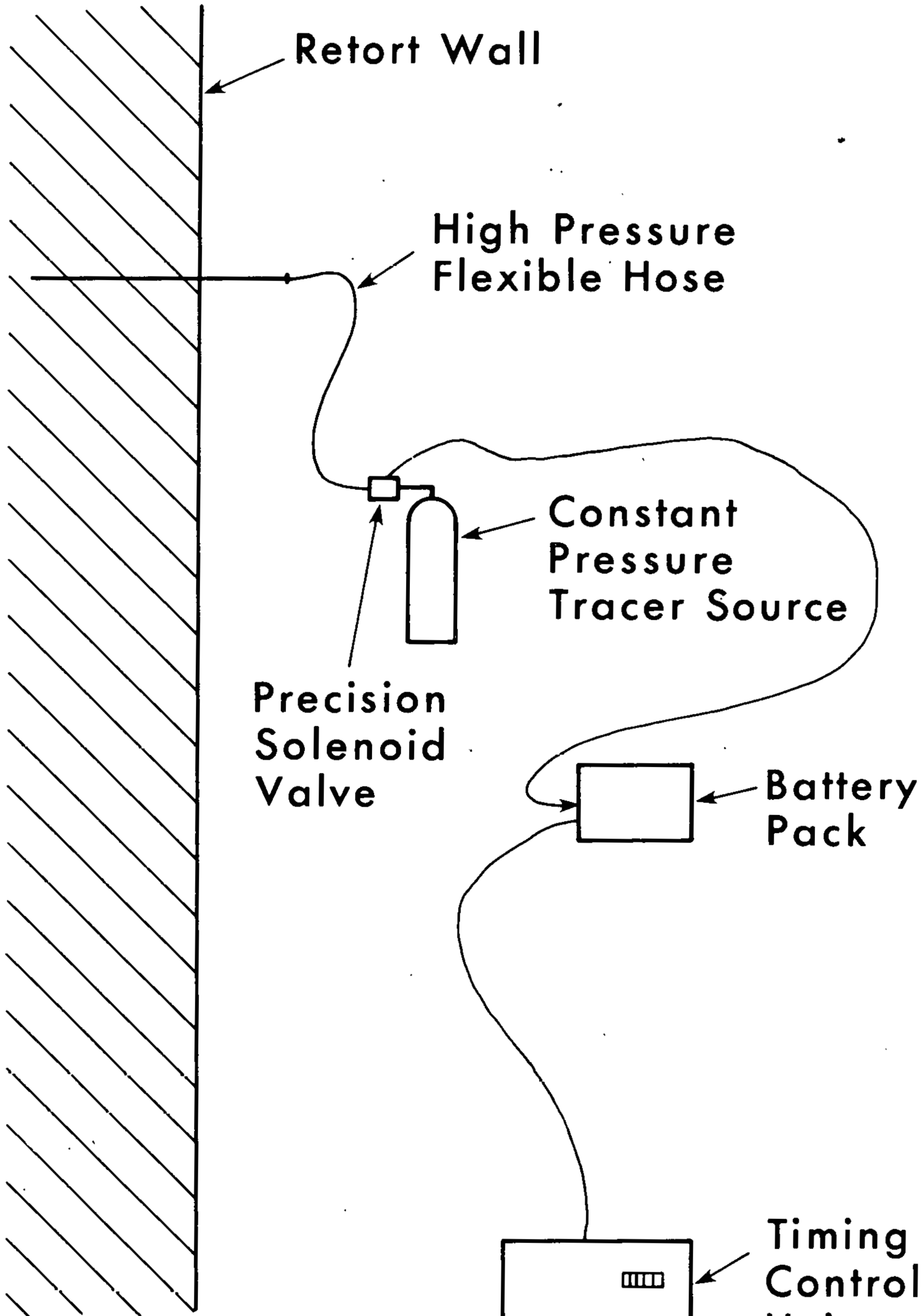

Figure 2. Tracer Injection System

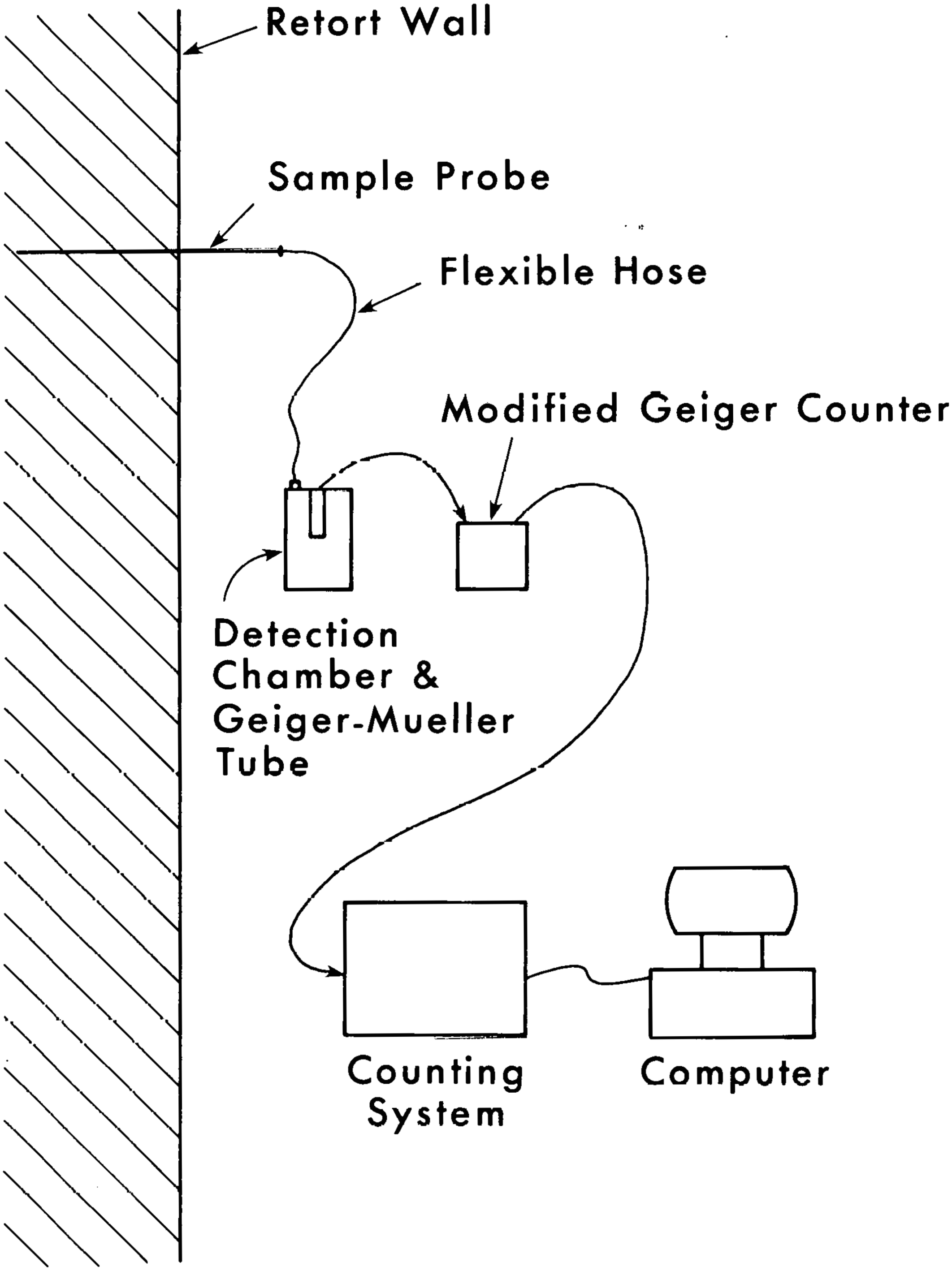

Figure 3. Tracer Detection System

In a detection chamber a Geiger-Mueller tube detects Kr-85 disintegrations. The signal is conditioned in the modified Geiger counter and is sent to the counting system where the counts are totaled over a preset interval. A computer calculates the characteristics of the tracer response curve using the count totals. Standard curve characteristics calculated are the area, first, second, and third moments, and the peak arrival time. Data printouts and graphs are output to the user.

The tracer test plan is designed to allow detailed velocity measurements in the region of the retort around the barrel at three superficial gas velocities (SGV). The superficial gas velocity is the volumetric flow rate divided by the cross-sectional area of the retort. Injections are made at the air inlet, at each sample tap on probe level 1 and at five sample taps A, D, F, H, and K on probe level 2. For each injection, twelve detection sample taps are monitored. Eleven of the detection sample taps are in one of the probe levels below the injection point and the twelfth tap is at the outlet. For example, to run a complete set of tests at one superficial gas velocity, four injections are made at the air inlet so that all four probe levels can be monitored. Three injections are made into each tap on probe level 1 and two injections are made into each of five taps on probe level 2. The resulting number of tests for each superficial gas velocity, excluding repeats and stage 1 tests, is forty seven. The number of injection-detection pairs of taps for each superficial gas velocity is more than five hundred.

Following the tracer tests, a steam flow test is conducted to estimate how a burn front would move through the retort. The steam test is run with an SGV of 0.0117 m/s of which 70 percent by volume is air and 30 percent by volume is steam. Both air and steam are heated to 112.8°C before entering the retort. Only heated air is introduced into the retort for the first four hours of the test to see if a low level fast moving thermal wave caused by the hot air can be detected (none was seen). After the initial four hours, steam is added to the air in the proportion stated above and the test is continued with no further changes in operating conditions.

MODELS

A computer program for modeling flow in porous media has been written by Bryan Travis of Los Alamos National Laboratories (LANL). This model uses a finite difference scheme to solve numerically equations for mass conservation, tracer concentration and conservation of momentum.(6) An early version of the Travis model has been applied, by Sandia National Laboratories (SNL), to modeling the 150 ton retort.(7) That version of the Travis model uses the Darcy flow equation

$$U = -(K/\mu) \quad (\nabla P - \rho g) \qquad (1)$$

where U, K, μ, ∇P, ρ and g are the SGV, permeability, fluid viscosity, pressure gradient, fluid density and gravitational acceleration respectively. This equation is a good approximation for low Reynolds number (Re), that is, for

$$Re = D_p \left| U \right| \rho/\mu\varepsilon \leqq 10 \qquad (2)$$

where D_p is the effective particle diameter, ε is the porosity and the other parameters are the same as in equation (1).

A copy of this version of the Travis model has been obtained from SNL and has been modified to include a refinement made by Travis. In the improved version of the model equation (1) has been changed to

$$U \left(1 + \frac{1.75 \, \rho \, D_p}{150 \, (1-\varepsilon)\mu} \left| U \right| \right) = -(K/\mu) \, (\nabla P - \rho g). \qquad (3)$$

Letting

$$K = \frac{\varepsilon^3 \, D_p{}^2}{150 \, (1-\varepsilon)^2} \qquad (4)$$

equation (3) becomes a form of Forchheimer's motion equation called Ergun's equation.[8] Ergun's equation is valid for a larger range of Reynolds number than is equation (1). Expressed as a function of Reynolds number, equation (3) is

$$U \left(1 + \frac{1.75\varepsilon}{150 \, (1-\varepsilon)} \, Re \right) = -(K/\mu) \, (\nabla P - \rho g). \qquad (5)$$

Note that for $\varepsilon<1$ (which must be the case)

$$\lim_{Re \to o} \; U \left(1 + \frac{1.75\varepsilon}{150(1-\varepsilon)} \, Re \right) = U \qquad (6)$$

which is the Darcy flow case (equation (1)). Ergun[9] and Minster and Fausett[10] discuss the origin, limitations and application of equation (3). Minster and Fausett discuss the use of a shape factor and other modifications to the Ergun equation. A shape factor is added to the Ergun equation by substituting $\phi_s D_p$ for D_p in equations (3) and (4). Based on data from 22 experiments on raw crushed oil shale Minster and Fausett have determined that $\phi_s = 0.47$ is an appropriate value. This value is used with both the Travis model and the Szekely model to be discussed below.

The input parameters for the Travis model are particle size, void fraction, permeability and either the top and bottom pressures or the velocity at the bottom of the retort. The output of the model is pressure and velocity as a function of position throughout the retort.

A flow model has been developed by Julian Szekely to simulate flow through blast furnace burdens.[11] This model uses a vectorial version of the Ergun equation to describe flow through packed beds with spatially varying void fraction and particle size. This model is used by Szekely and others to study a large variety of rubble bed packing arrangements.[11,12,13] The results indicate that the model works well, if modifications are made for void defects near walls and for low permeability interfaces between areas of different particle sizes.[14] These modifications will be incorporated if the basic model shows qualitative agreement with experiments.

The input parameters for this model include gas flow rate, and the spatial arrangement of particle sizes and void fractions. The values output by the model include the overall pressure drop, stream function values, and pressures and velocities in all areas of the rubble bed.

DISCUSSION

Tracer Data

The tracer test data are in the form of tracer concentration as a function of elapsed time since injection. Typical tracer response curves are shown in figures 4 and 5. Note that both examples have obvious peaks and that the decay time is longer than the rise time. Since the response curve in figure 4 has a lower concentration than the curve in figure 5, the random noise is more apparent. In many cases this becomes an important factor. For example, if an analysis based on the mean residence time, variance, and skewness (1st, 2nd and 3rd moments respectively) of the response curve is desired, the noise level can seriously affect the values obtained by exaggerating the weight of the tail region of the curve. The use of curve fitting techniques can reduce the noise problem by approximating the response curve with an acceptable curve shape. However, the validity of this method of analysis depends on selecting the proper parameters to represent the system. The objective of this study is to compare tracer response data with steam flow data and model predictions. Tracer velocities are used for

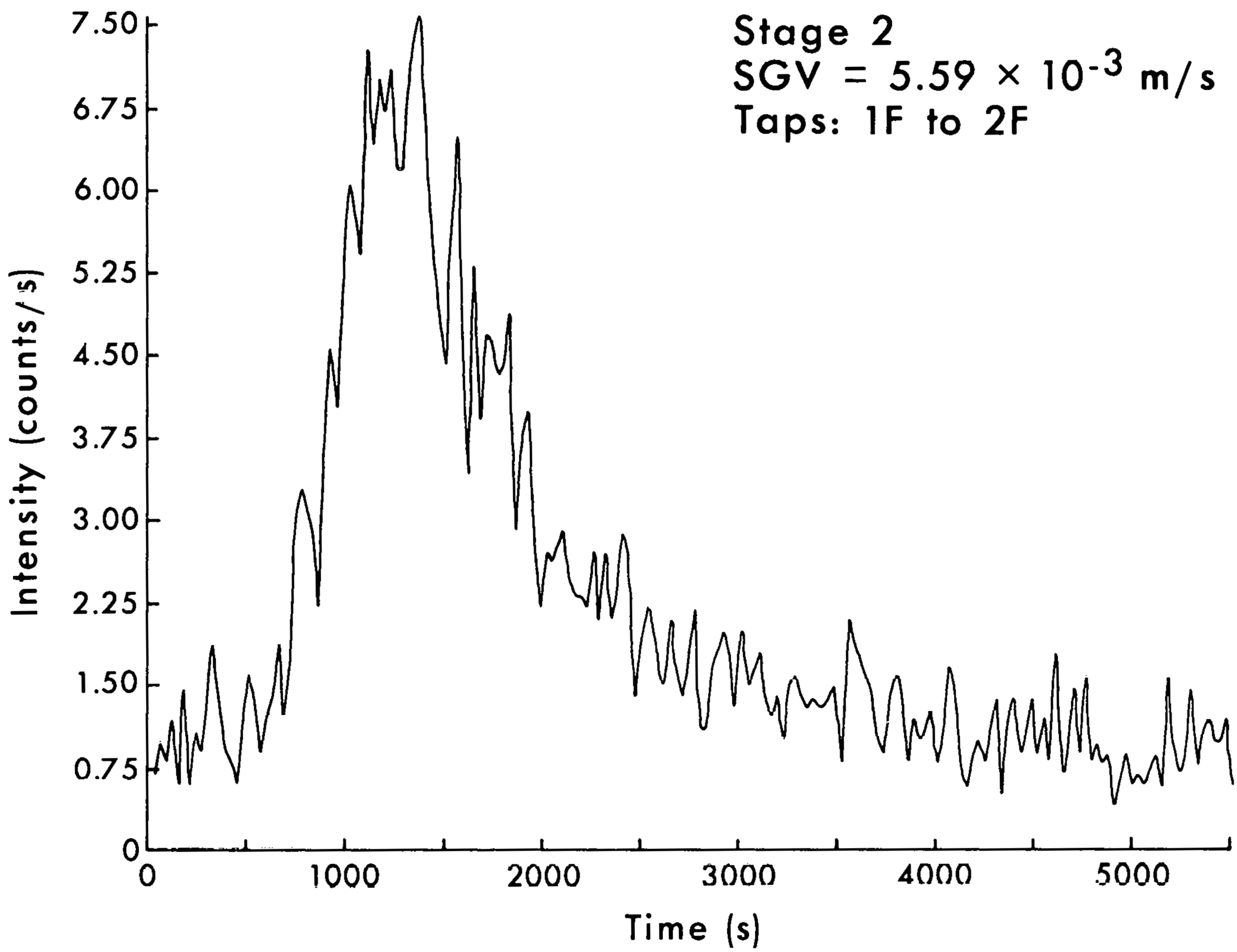

Figure 4. Typical Tracer Response for Low Concentration

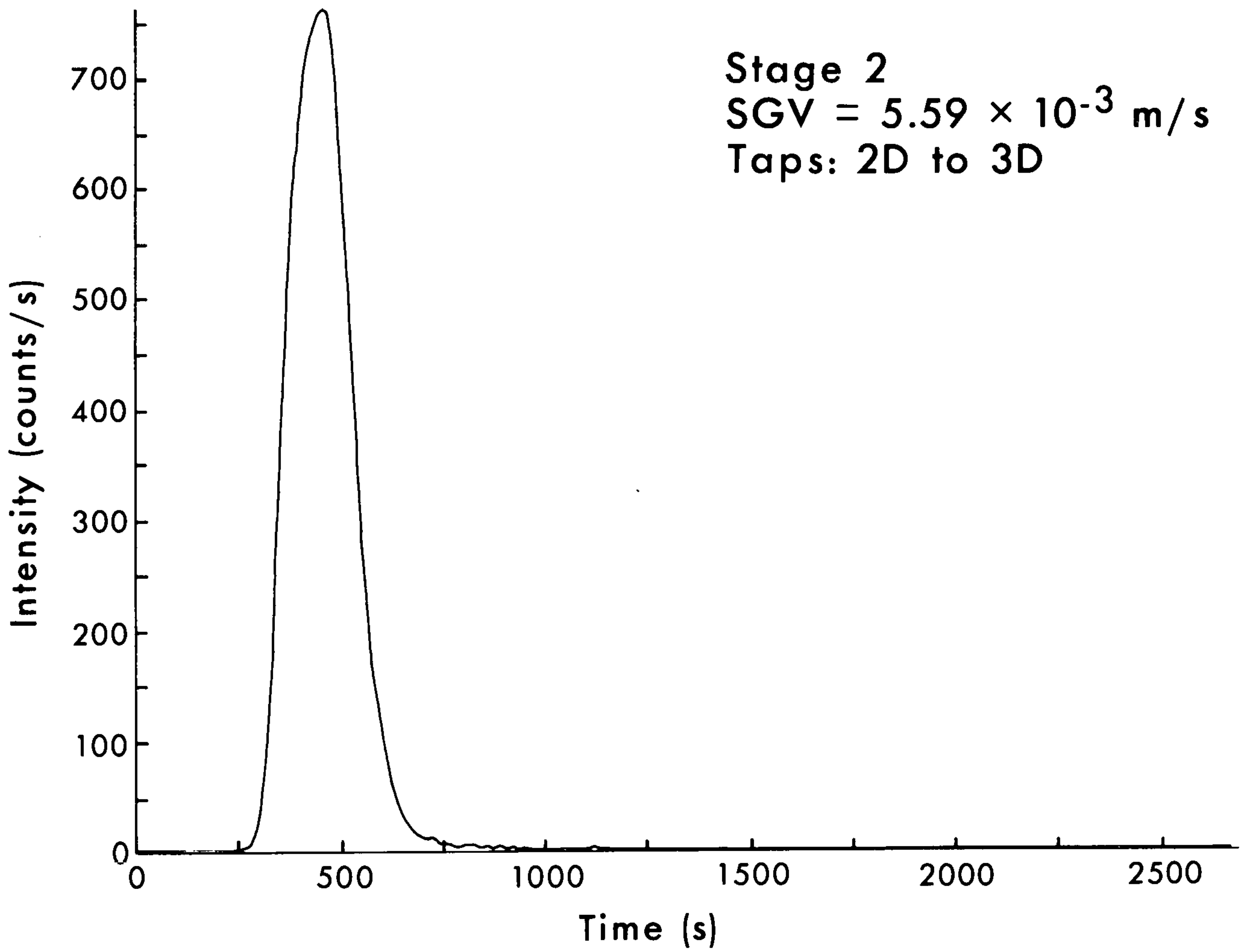

Figure 5. Typical Tracer Response

the comparisons. No effort is made to analyze the curve shapes resulting from the tracer tests except where multiple peaks are apparent.

The multiple peak phenomenon is seen in several of the response curves. Examples are shown in figures 6 through 9. In most cases the double peaks are seen when injection and detection taps are adjacent to the retort walls. This may be indicative of a higher rubble void fraction near the wall which causes a relatively direct flow path compared to tortuous flow through the rubble bed. To investigate this possibility, the response curve shown in figure 6 has been analyzed using the Ergun equation to determine the relationship between the void fractions of the two regions. The Ergun equation is applied to each of the two regions using the assumption that fluid viscosity, shape factor, particle size and fluid density are the same for each region. Since the pressure drop between the injection point and the detection point must be the same for each path, the two equations can be combined resulting in the desired relationship between the void fractions in the two regions. Obviously, the two void fractions can not be obtained independently, but a reasonable value for the rubble void fraction can be used to produce an estimate of the void fraction near the wall. Using the average bed void fraction, 0.472, for the rubble bed void fraction results in an estimate of 0.904 for the void fraction along the wall.

In some cases where tests have been repeated, two distinct types of response curves result. Figure 10 shows one example of this effect. One of the response curves, A, has a double peak, probably indicating a flow channel along the wall. The other response curve, B, shows only

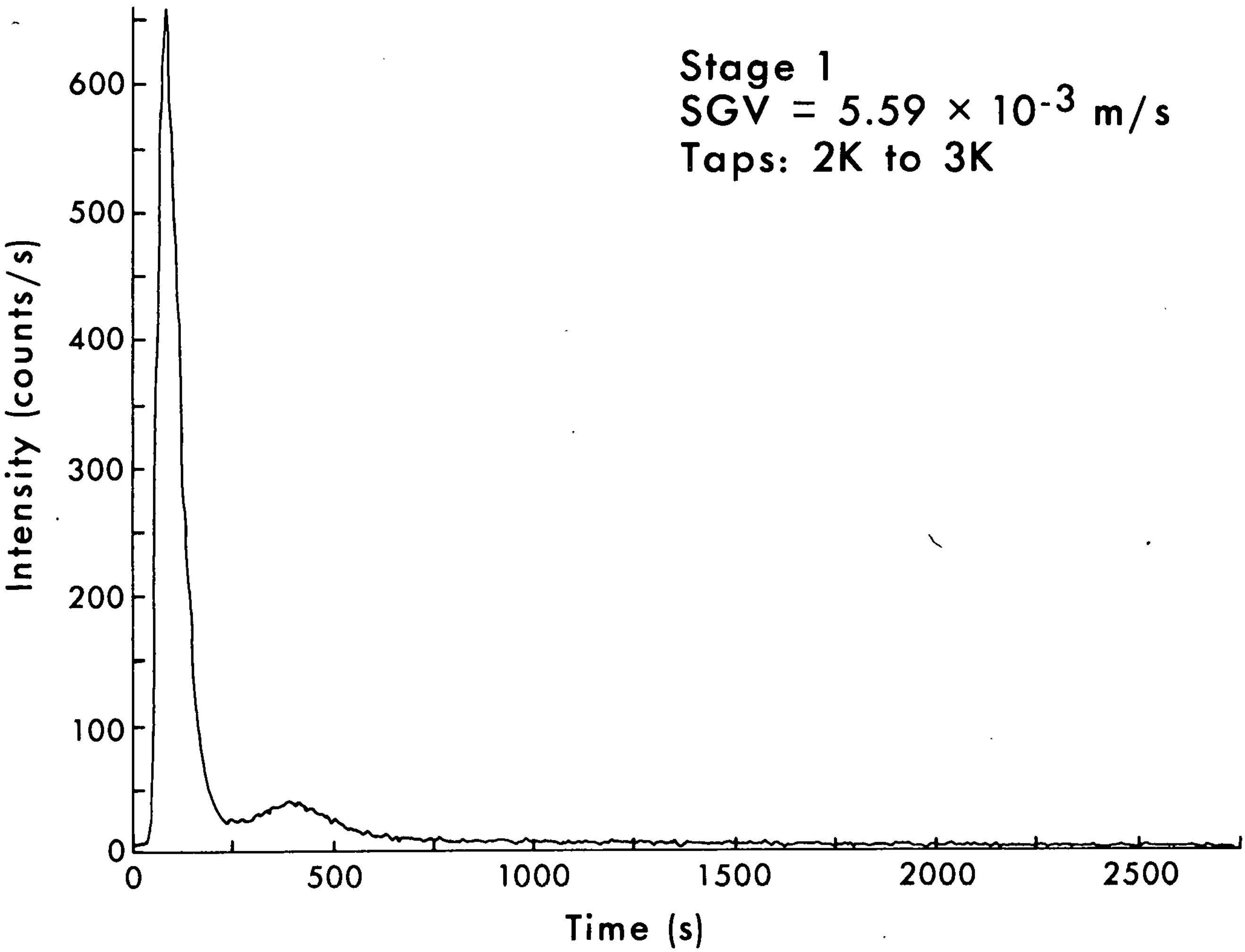

Figure 6. Multiple Peak Tracer Response

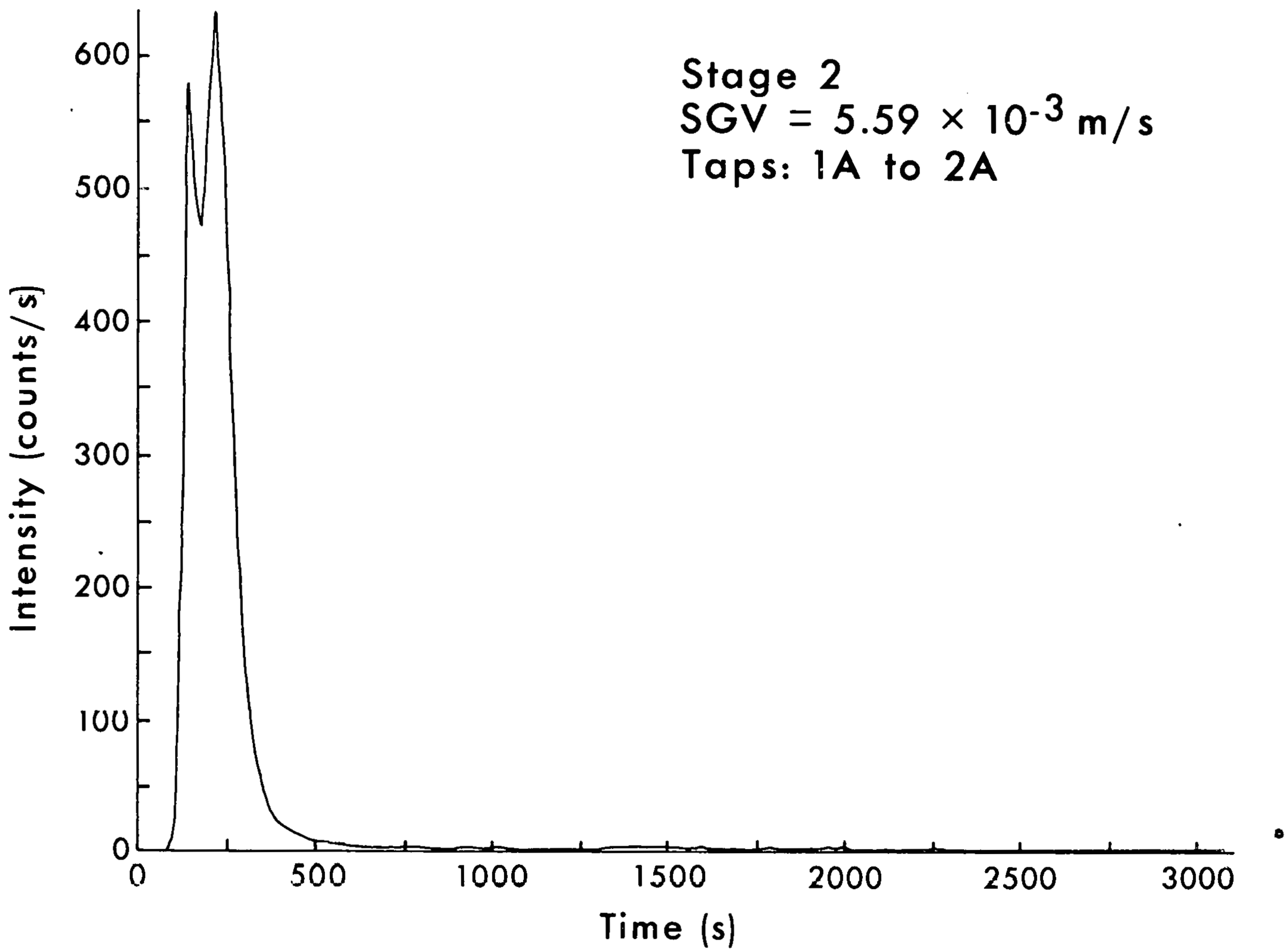

Figure 7. Multiple Peak Tracer Response

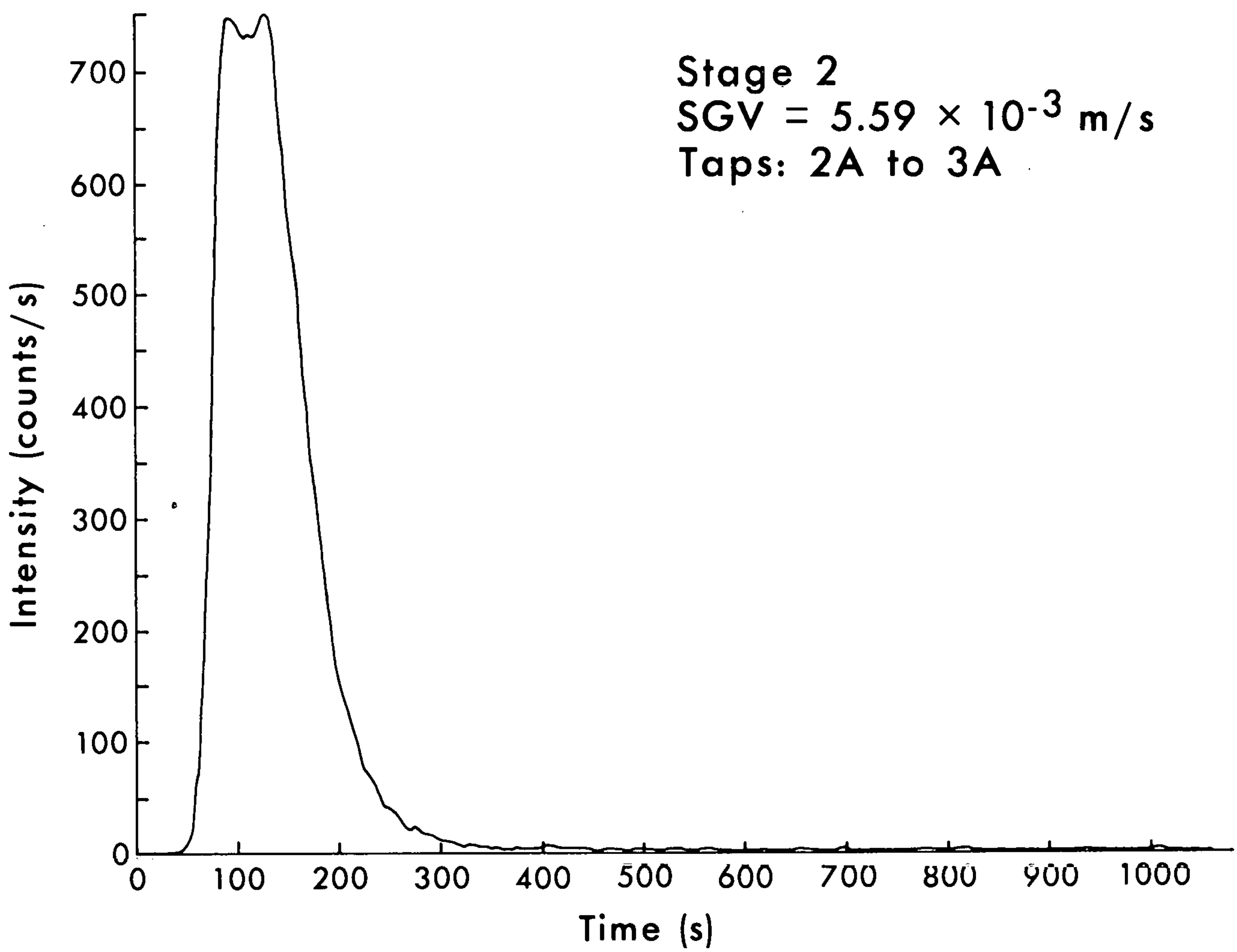

Figure 8. Multiple Peak Tracer Response

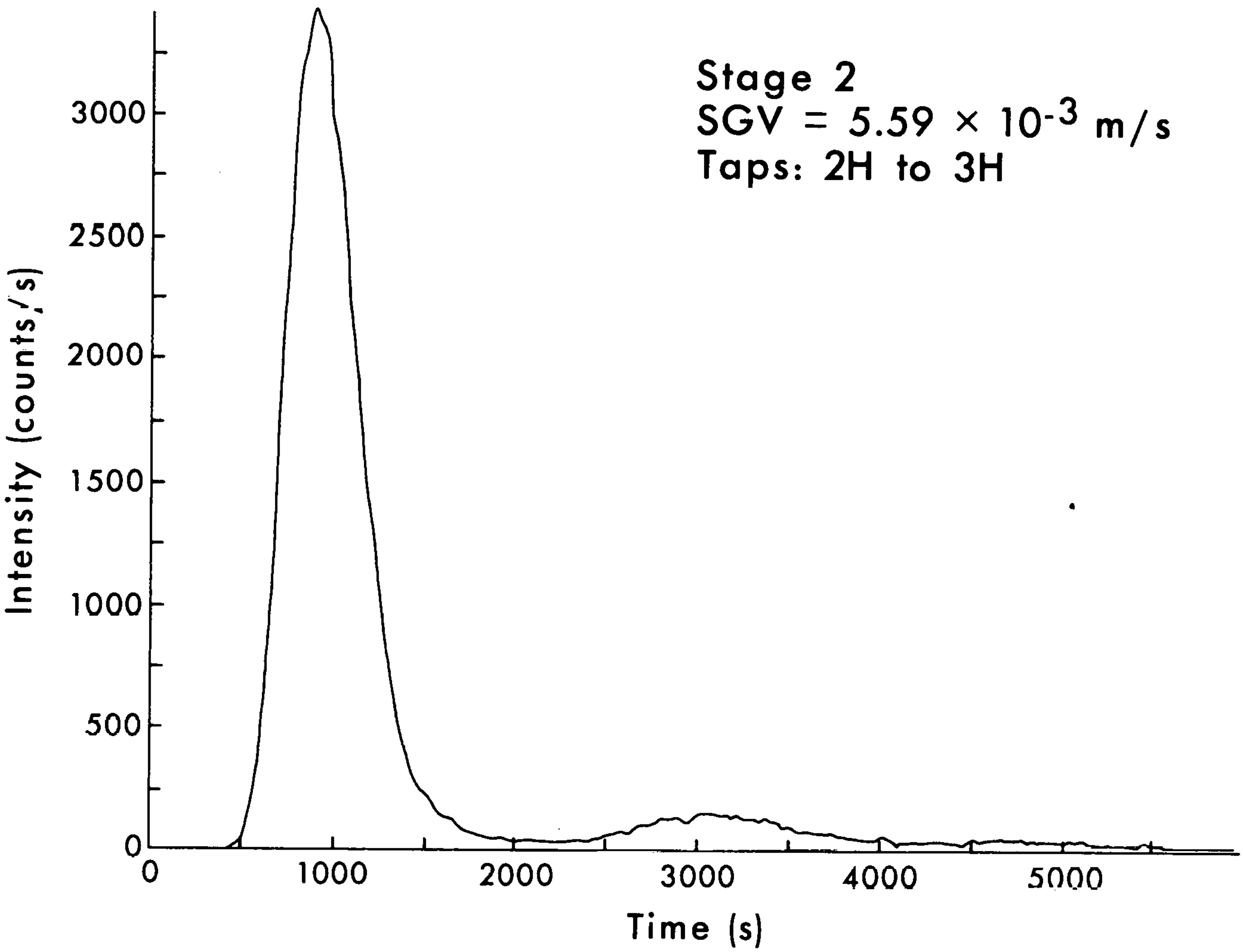

Figure 9. Multiple Peak Tracer Response

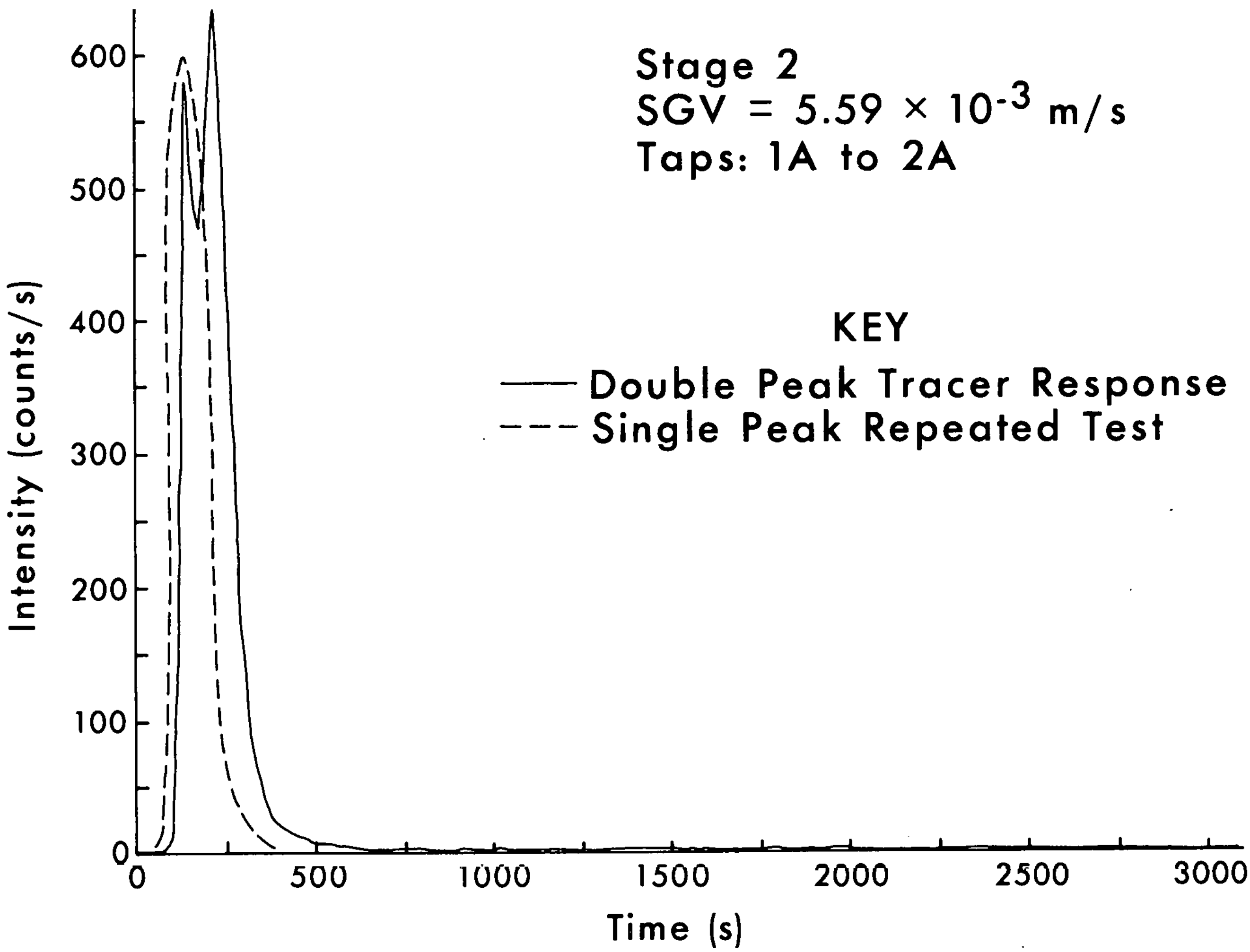

Figure 10. Inconsistent Tracer Response

one peak, but the response time of this peak is nearly the same as the response time of the first peak of curve A. This effect may also be due to the nearness of the wall. Slight variations in injection pressures or volumes, or rubble bed settling could direct the tracer towards or away from the wall causing single or double peaks. Since the rubble bed geometry below the injection taps is not known in detail, no further analysis of this effect is possible.

The tracer response times are converted into an apparent velocity by dividing the straight line distance between the injection and detection points by the response time. A plot of the apparent tracer velocity versus the superficial gas velocity for stage 2 inlet to outlet tracer tests is shown in figure 11. The expected SGV/ε is also shown. The reason for the low tracer velocity at the higher superficial gas velocity is not known. In an effort to see if this effect is general, similar plots have been prepared for tracer velocities between adjacent vertical taps in the rubble bed. The plots for the stage 1 tests are shown in figure 12 and the plots for the stage 2 tests are shown in figures 13 through 15. Most of the curves show the same effect at the higher superficial gas velocity.

Model Data

Comparing the flow model predictions with the tracer test results is complicated by uncertainty about the rubble bed configuration. Both the Travis and Szekely models use the Ergun equation (3) to relate the

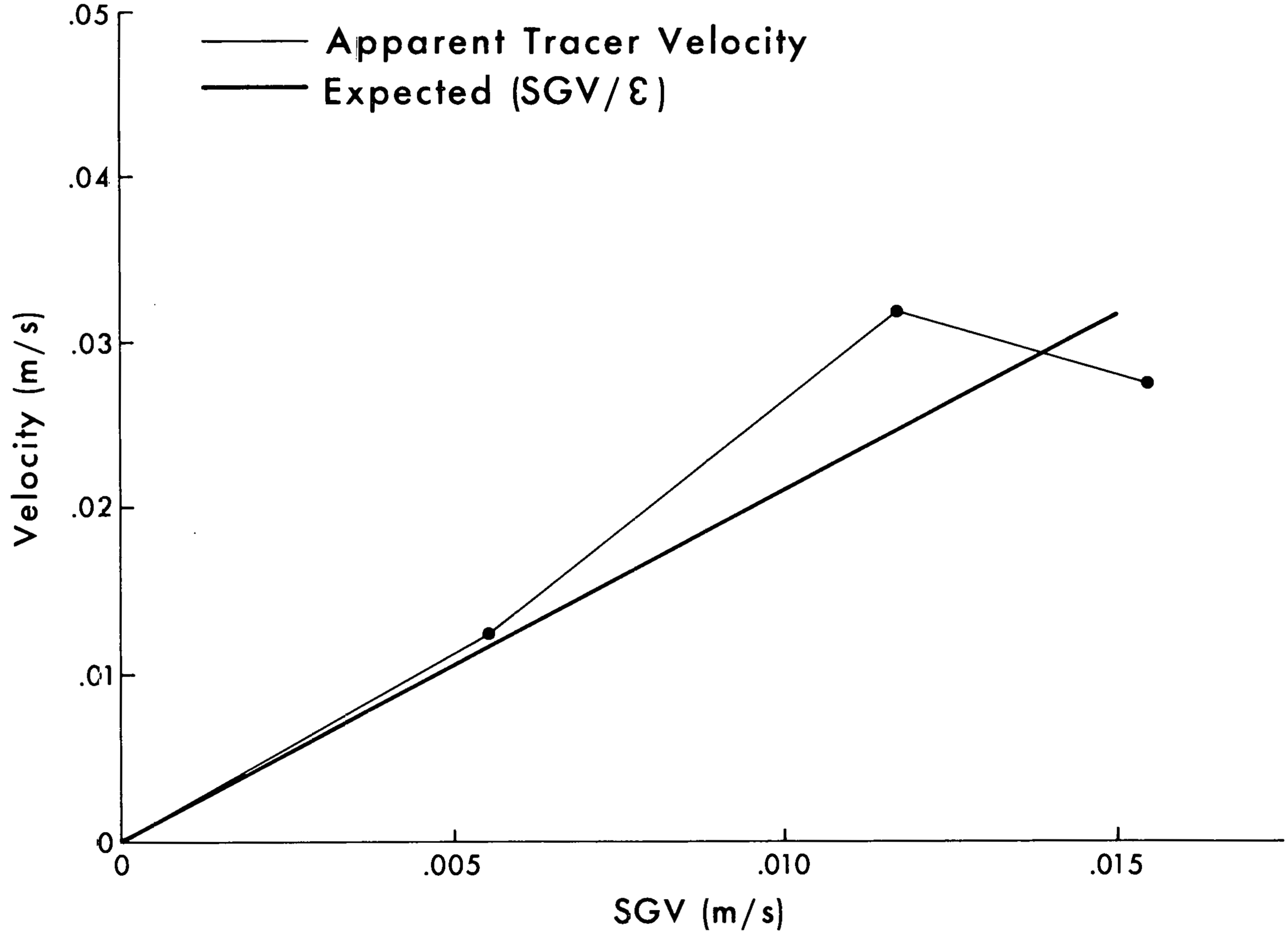

Figure 11. Inlet to Outlet Velocity, Stage 2

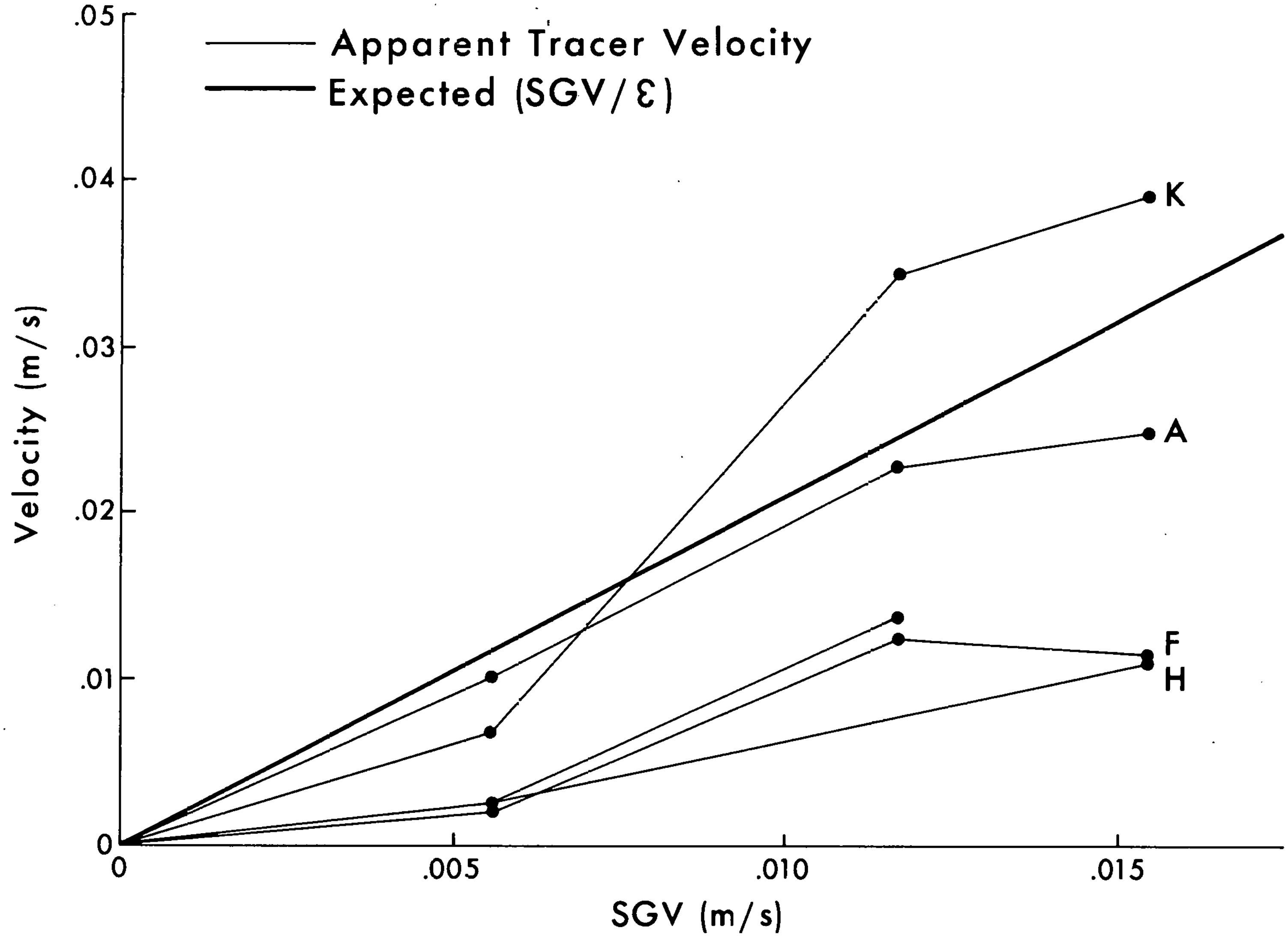

Figure 12. Level 2 to Level 3 Velocity, Stage 1

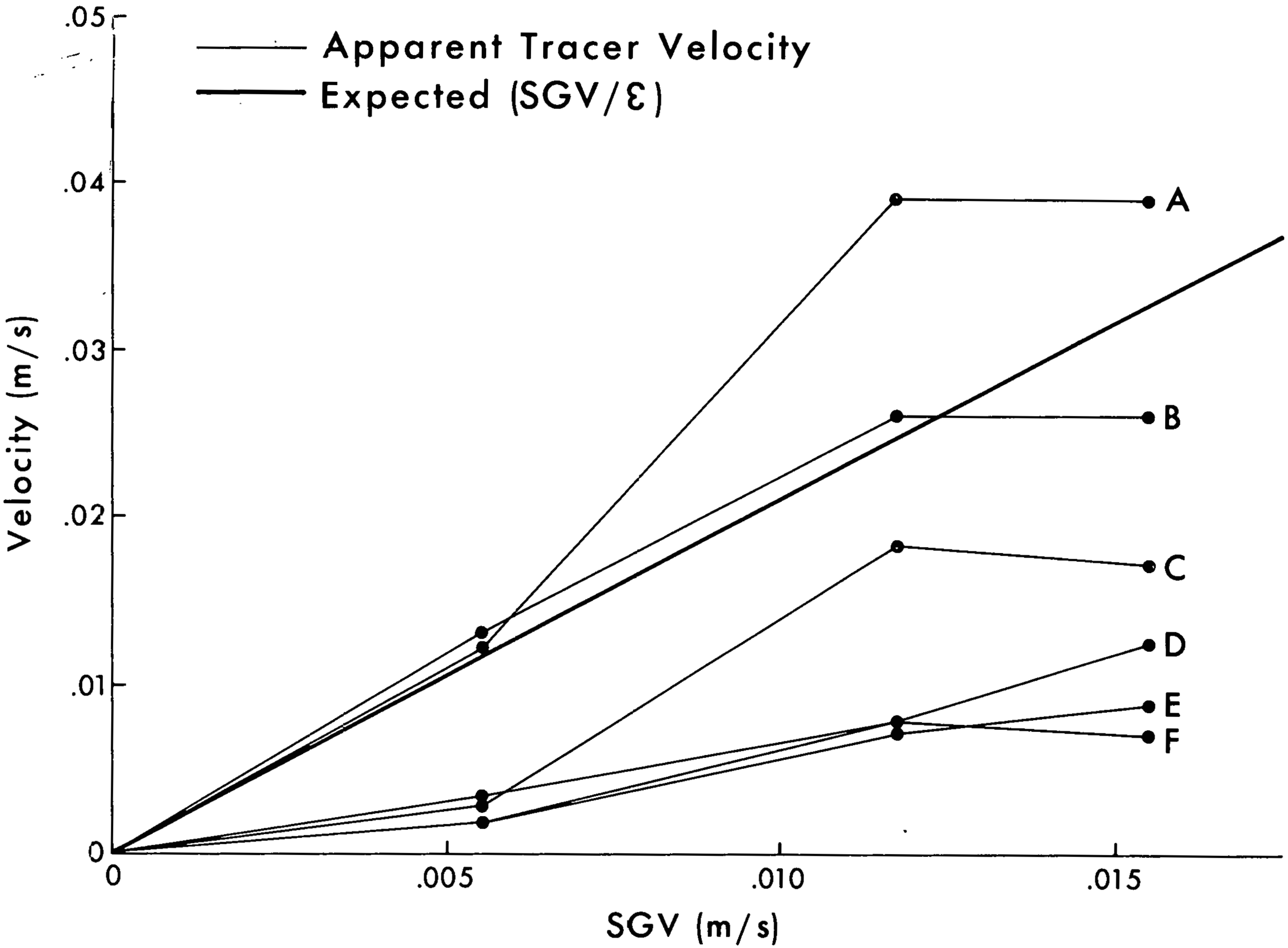

Figure 13. Level 1 to Level 2 Velocity, Taps A through F, Stage 2

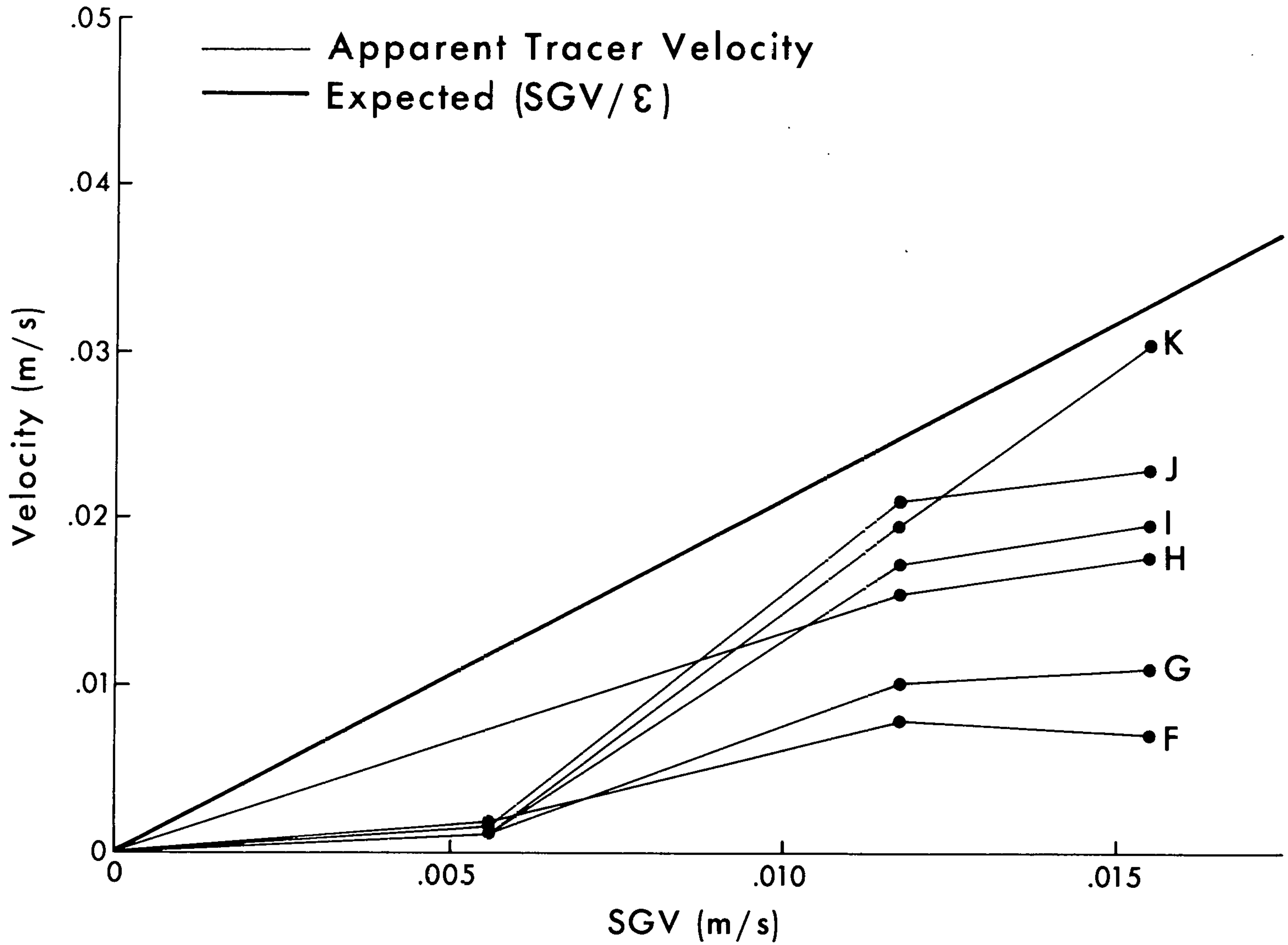

Figure 14. Level 1 to Level 2 Velocity, Taps F through K, Stage 2

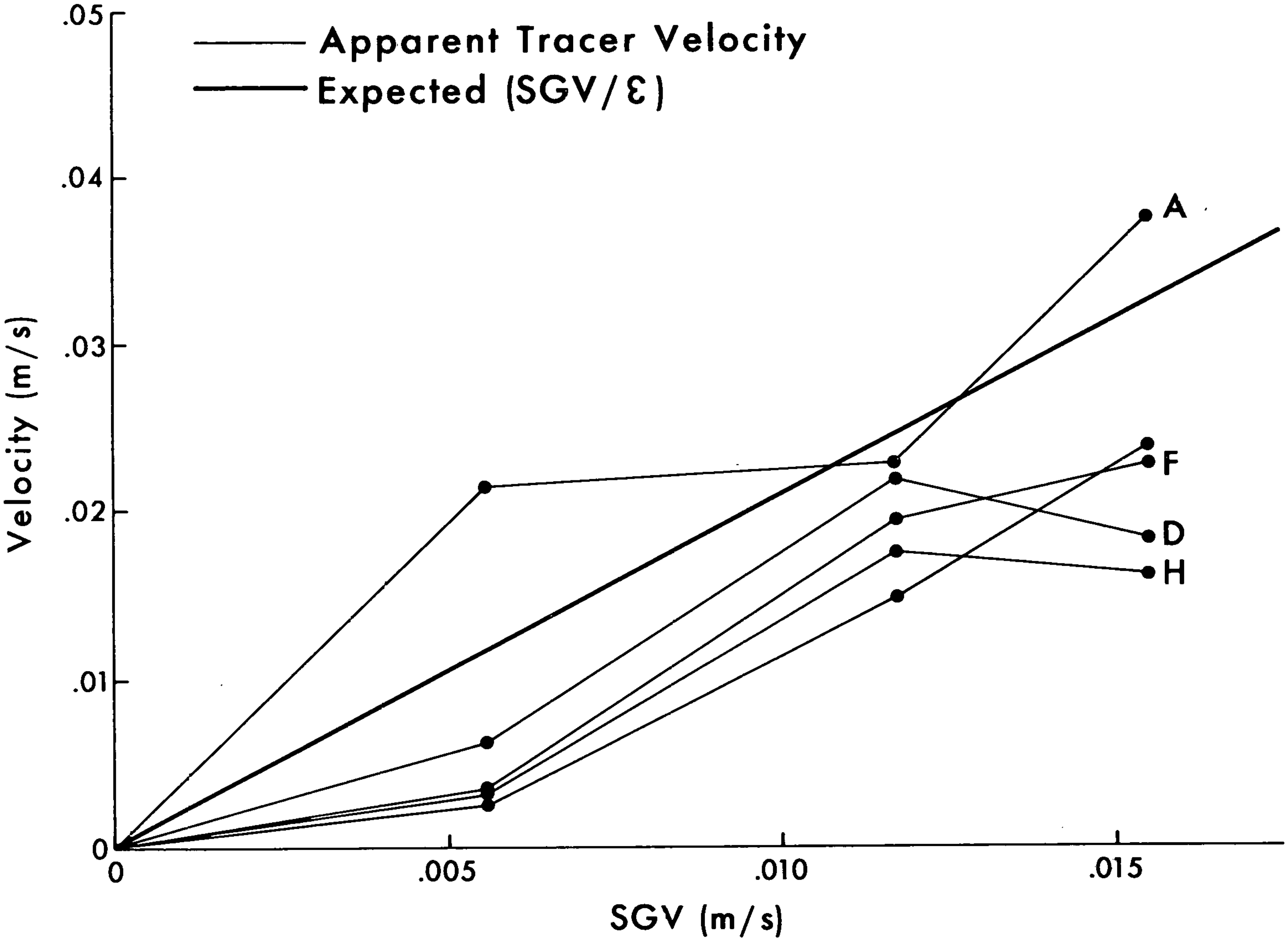

Figure 15. Level 2 to Level 3 Velocity, Stage 2

velocity with the pressure gradient. This equation requires that the bed parameters ε and D_p be spatially uniform (4). Ergun's equation in differential form can be used for cases where these parameters vary in a known manner, but random variation can be treated only in a statistical sense. Since the rubble bed configuration is (to some degree) uncertain, the effect of spatial variation of ε and D_p should be considered. A sensitivity analysis has been made in order to demonstrate the effect of this uncertainty on the validity of the model calculations.

Specifically the sensitivity of K (equation (4)) with respect to ε and D_p is of interest. By definition these sensitivities are respectively

$$S_{\varepsilon}^{K} \triangleq \lim_{\Delta\varepsilon \to 0} \frac{\Delta K/K}{\Delta\varepsilon/\varepsilon} = \frac{\varepsilon}{K}\frac{\partial K}{\partial \varepsilon} \tag{7}$$

and

$$S_{D_p}^{K} \triangleq \lim_{\Delta D_p \to 0} \frac{\Delta K/K}{\Delta D_p/D_p} = \frac{D_p}{K}\frac{\partial K}{\partial D_p} \tag{8}$$

Equation (7) says that the sensitivity of K with respect to ε is the fractional (or percent) change in K divided by the fractional (or percent) change in ε for vanishing small changes in ε with D_p constant. A corresponding statement can be made for equation (8). Applying these definitions to equation (4) yields

$$S_{D_p}^{K} = 2 \tag{9}$$

and

$$S_{\varepsilon}^{K} = 3 + \frac{2\varepsilon}{1-\varepsilon} \quad . \tag{10}$$

The change ΔK can be approximated using the total differential of K. The approximation is

$$\Delta K \cong \frac{\partial K}{\partial D_p} \Delta D_p + \frac{\partial K}{\partial \varepsilon} \Delta\varepsilon \ . \tag{11}$$

Substituting sensitivities into equation (11) and dividing by K we have, for small changes in ε and D_p, the fractional change in K

$$\frac{\Delta K}{K} \cong 2 \frac{\Delta D_p}{D_p} + \left(3 + \frac{2\varepsilon}{1-\varepsilon} \right) \frac{\Delta\varepsilon}{\varepsilon} \ . \tag{12}$$

In particular, if the fractional change in D_p and ε is 0.1 and if the nominal $\varepsilon = 0.472$ the effect on K is a fractional change of approximately 0.68 or 68%.

To illustrate the presence of spatial nonuniformities tracer and model calculation results have been converted to apparent velocities and normalized by dividing the velocities by SGV/ε. The normalized data from the stage 1 tracer tests are plotted as a function of radial position in figures 16 through 18. Note that the velocities near the center of the retort are lower than the velocities near the retort walls. The model predictions correspond to a normalized velocity of 1.0 for all radial positions. Figure 16 shows that, for the sample point orientation being used, there is not a material balance. Both sides of the retort have

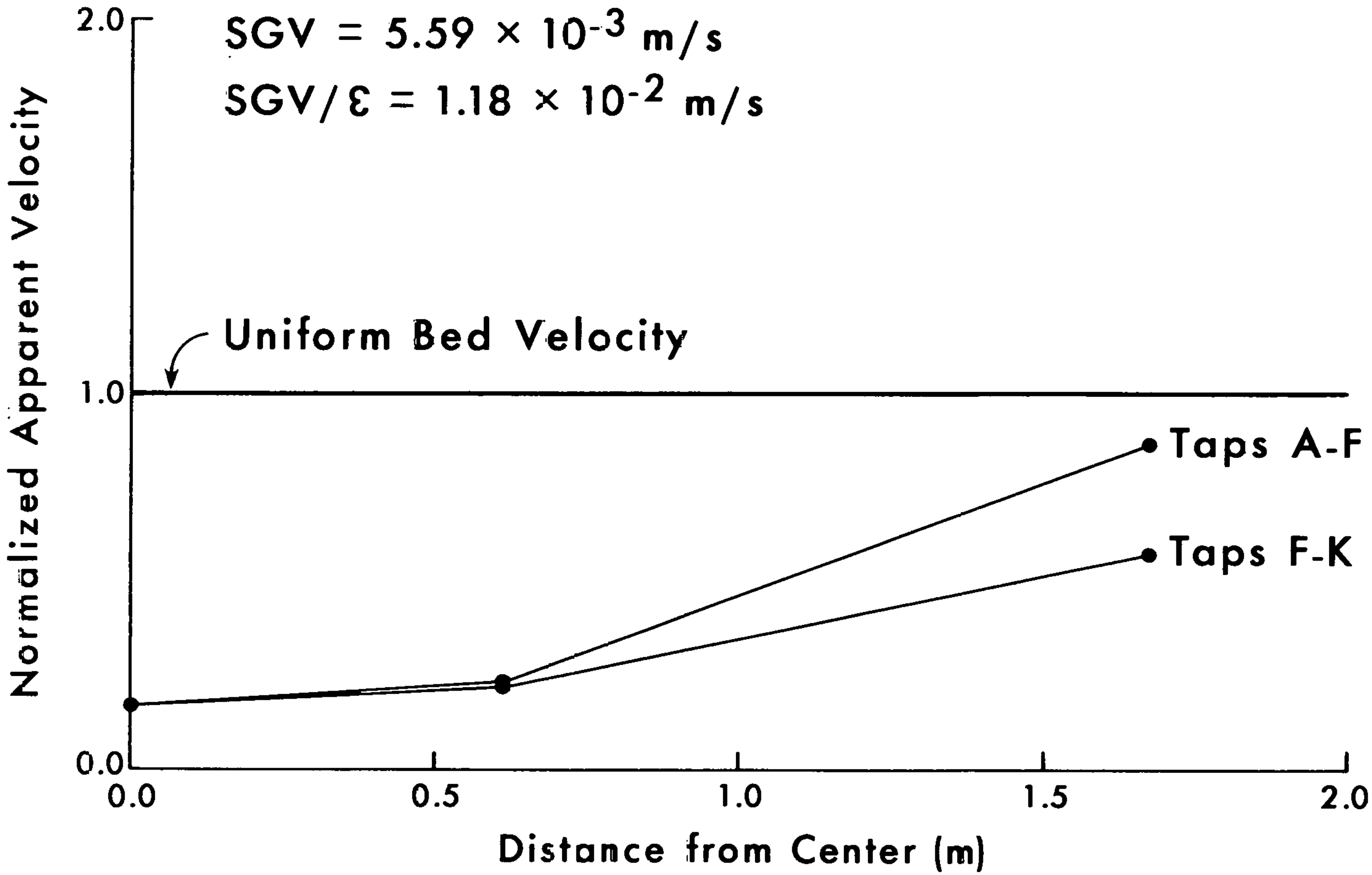

Figure 16. Level 2 to Level 3 Normalized Apparent Velocity, Stage 1

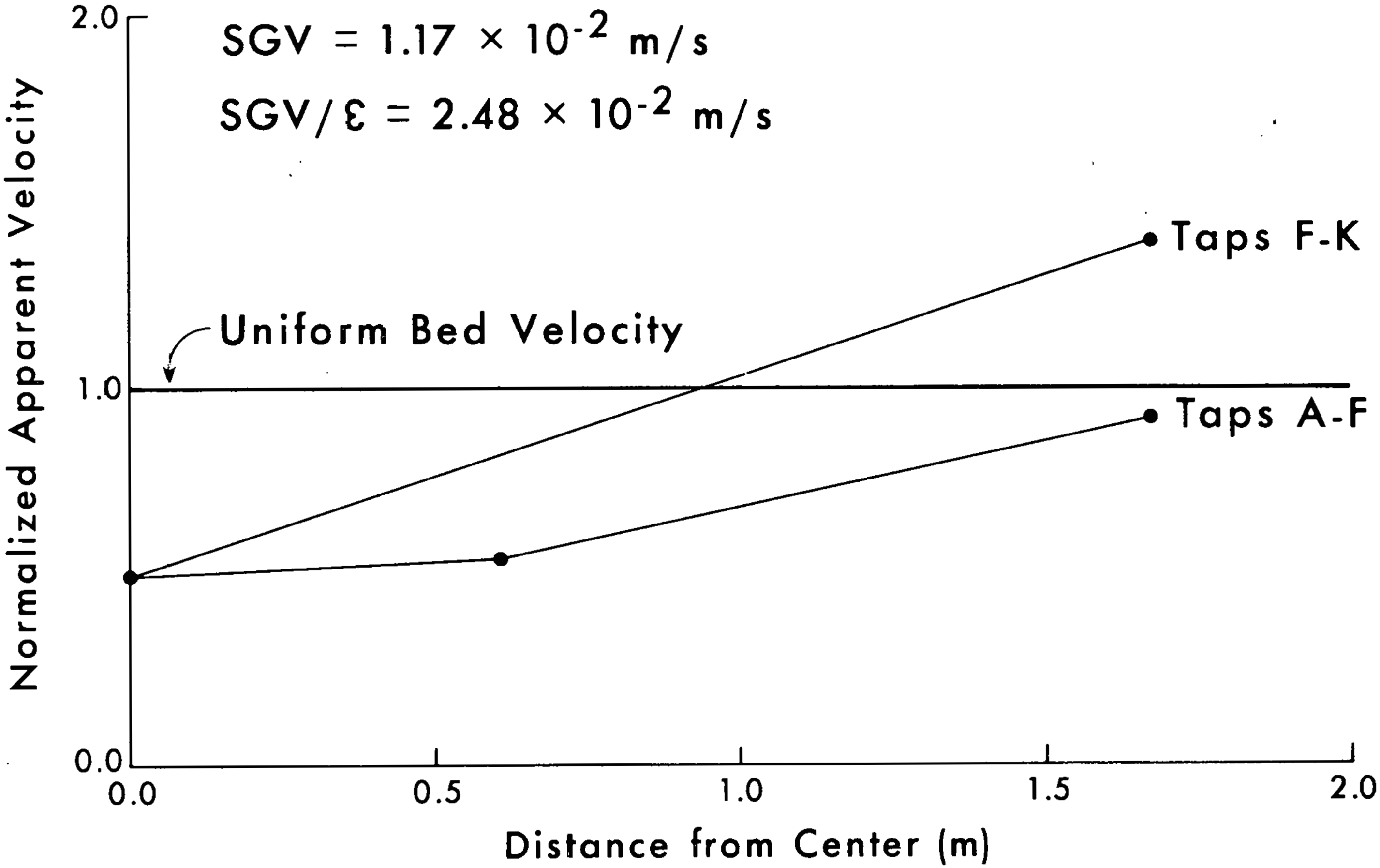

Figure 17. Level 2 to Level 3 Normalized Apparent Velocity, Stage 1

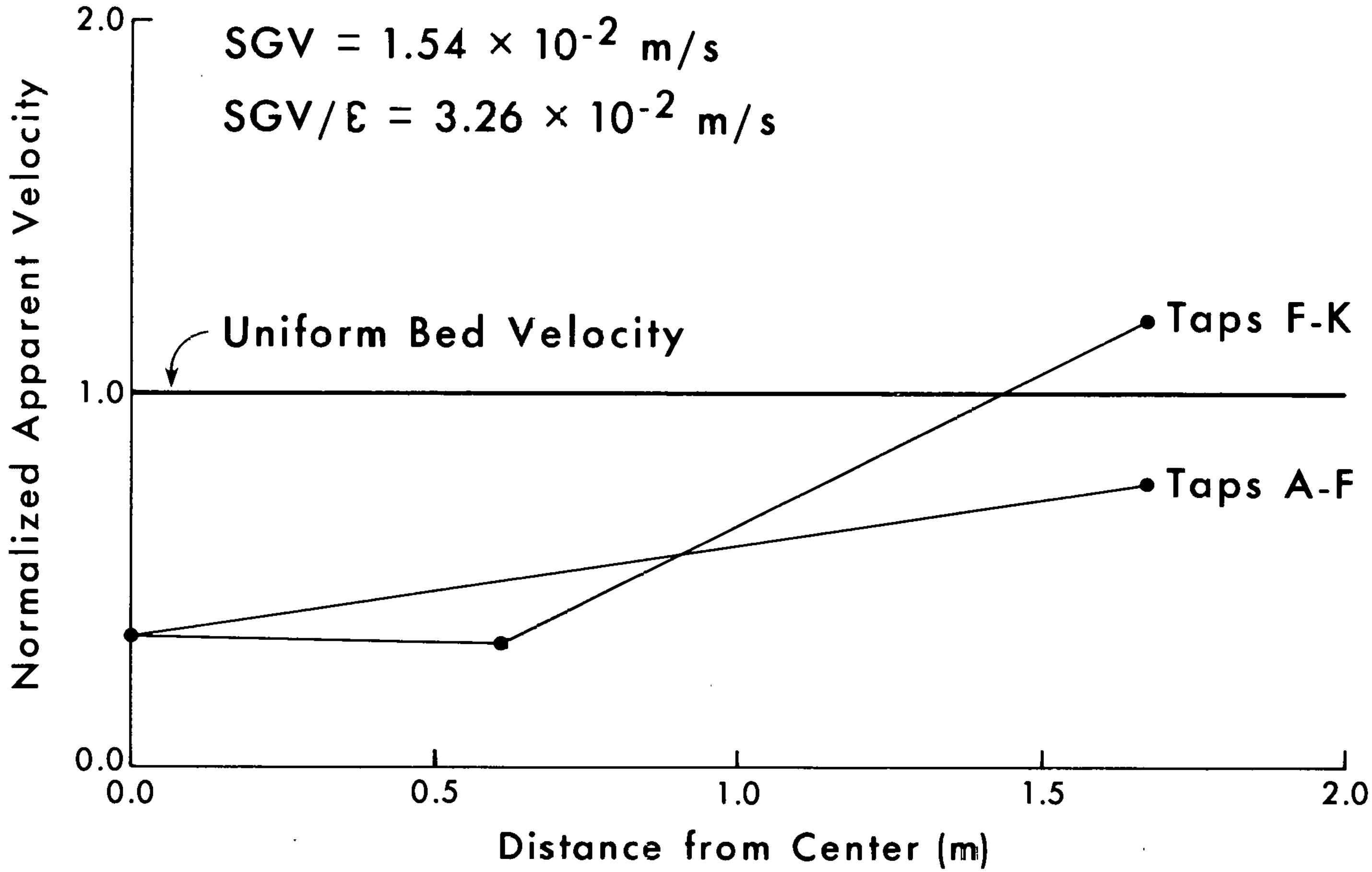

Figure 18. Level 2 to Level 3 Normalized Apparent Velocity, Stage 1

lower velocities than are necessary to account for all the air moving through the retort. Since there is no obstruction in the retort during the stage 1 tests, the nonuniform velocity distribution and the lack of mass balance must be the result of bed nonuniformities.

Normalized apparent velocities calculated from the stage 2 tracer tests are plotted as a function of radial position in figures 19 through 24. In figures 21 through 24 values calculated from the two flow models are also plotted. Because of the different interpolation techniques necessary for the two flow models, some end effects appear when velocity calculations are made near the walls or the centerline of the retort. However, for velocities away from the walls and the centerline, the two models are in good agreement. For velocities between probe level 1 and probe level 2 the models predict uniform velocities at radii greater than 0.61 meters and lower velocities nearer the center of the retort. The tracer tests show a more pronounced difference in velocities, with very low velocities near the center of the retort and high velocities near the wall. Tests at all superficial gas velocities show the same general characteristics. For velocities between probe levels 2 and 3, the models predict uniform velocities across the bed and the tracer tests show nearly uniform velocities for the 0.0117 SGV. At SGV's of 0.0056 and 0.0154 m/s, however, there are again the low velocities at the center of the retort and high velocities at the walls.

To compare stage 1 data with stage 2 data, the stage 2 velocities between probe levels 2 and 3 have been divided by the stage 1 velocities at the same positions. The plot of the resulting values at an SGV of

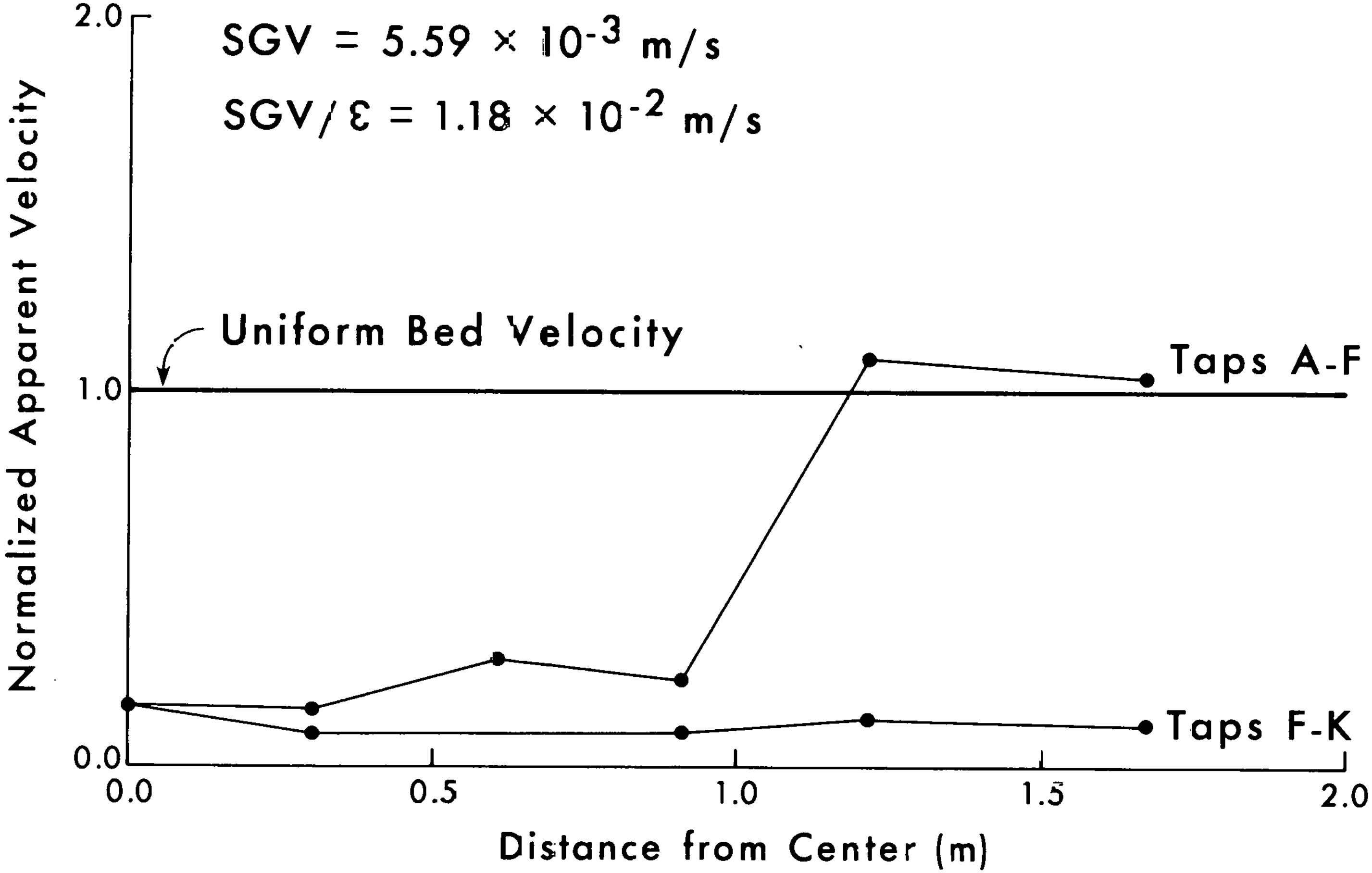

Figure 19. Level 1 to Level 2 Normalized Apparent Velocity, Stage 2

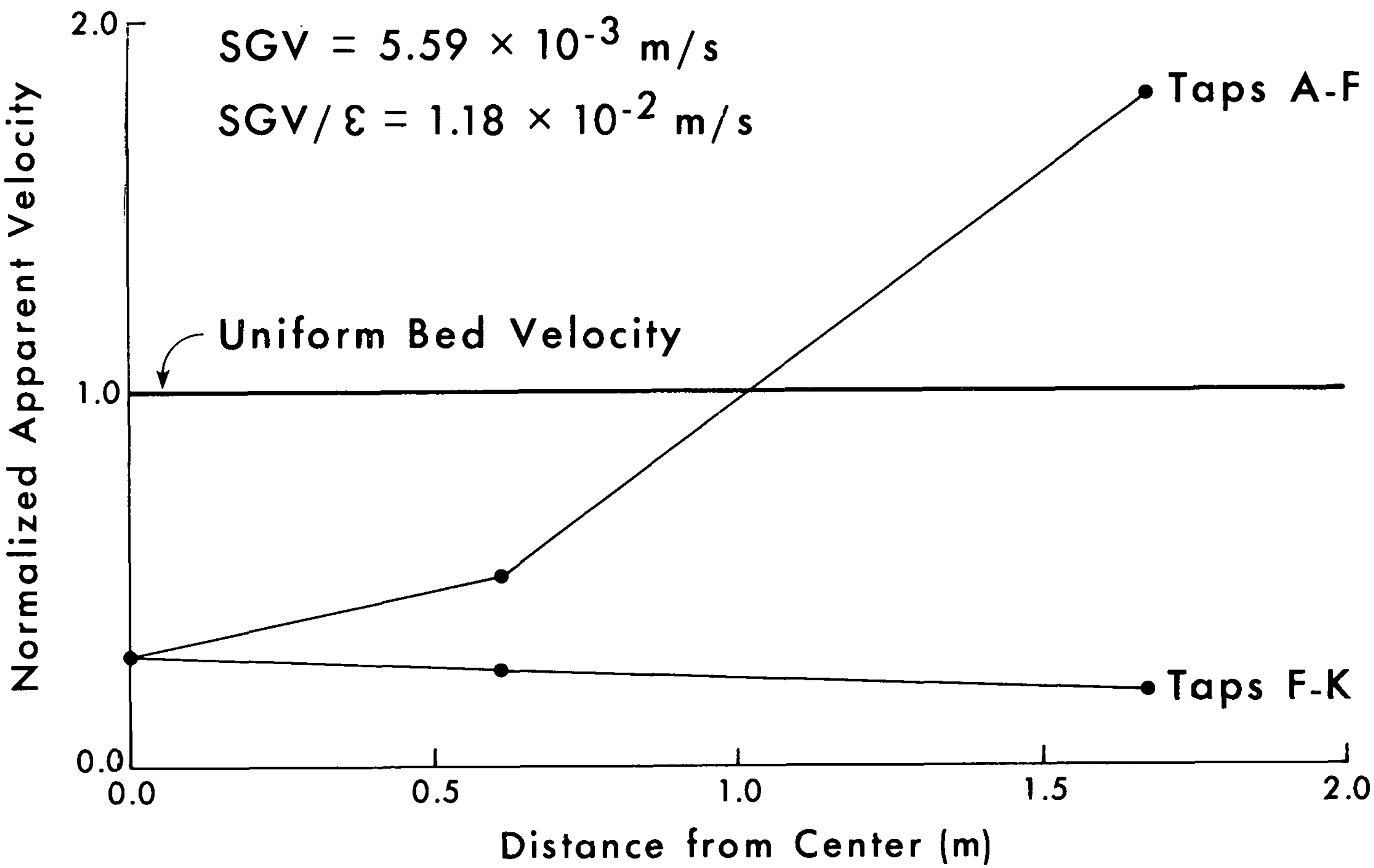

Figure 20. Level 2 to Level 3 Normalized Apparent Velocity, Stage 2

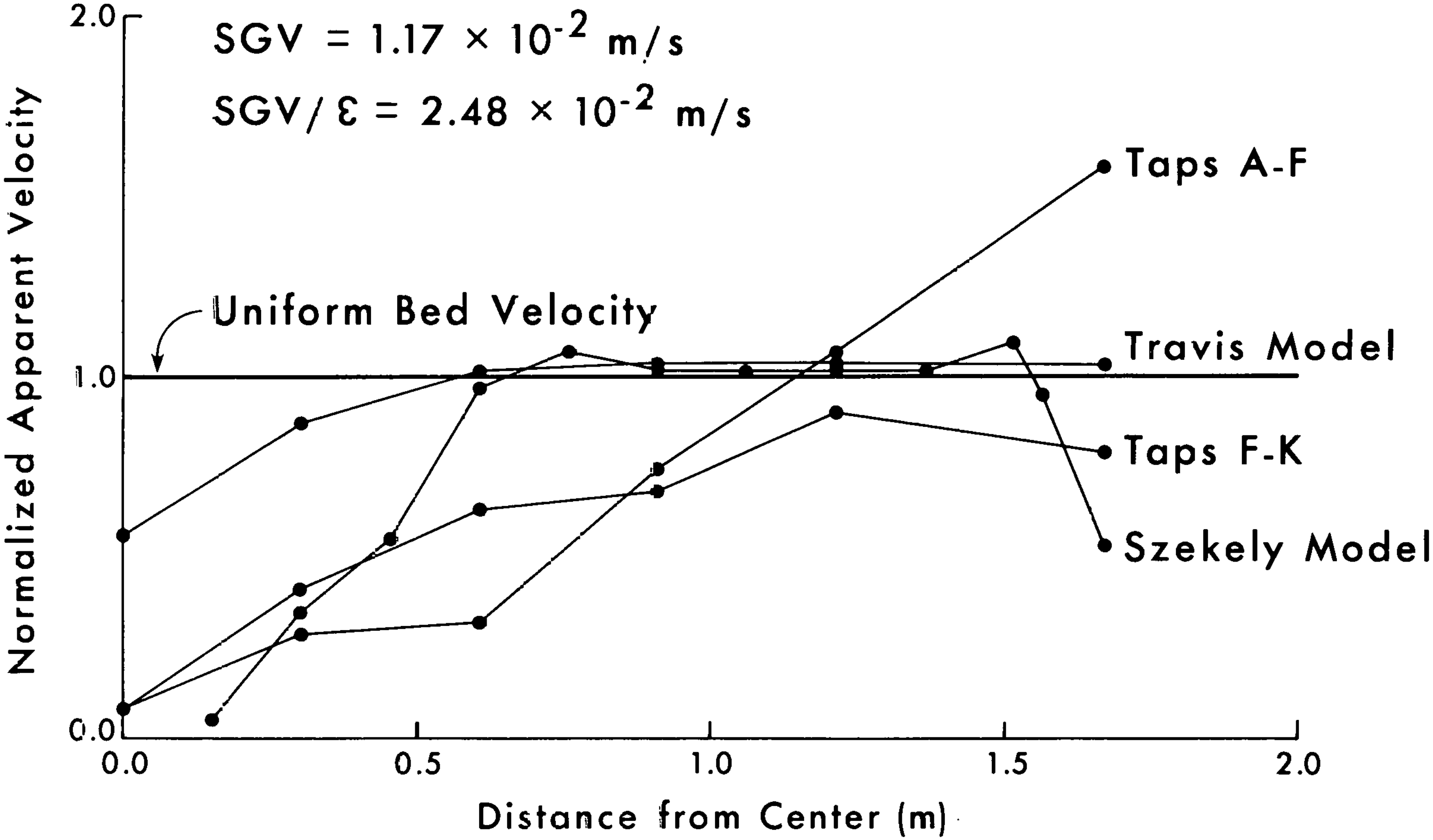

Figure 21. Level 1 to Level 2 Normalized Apparent Velocity, Stage 2

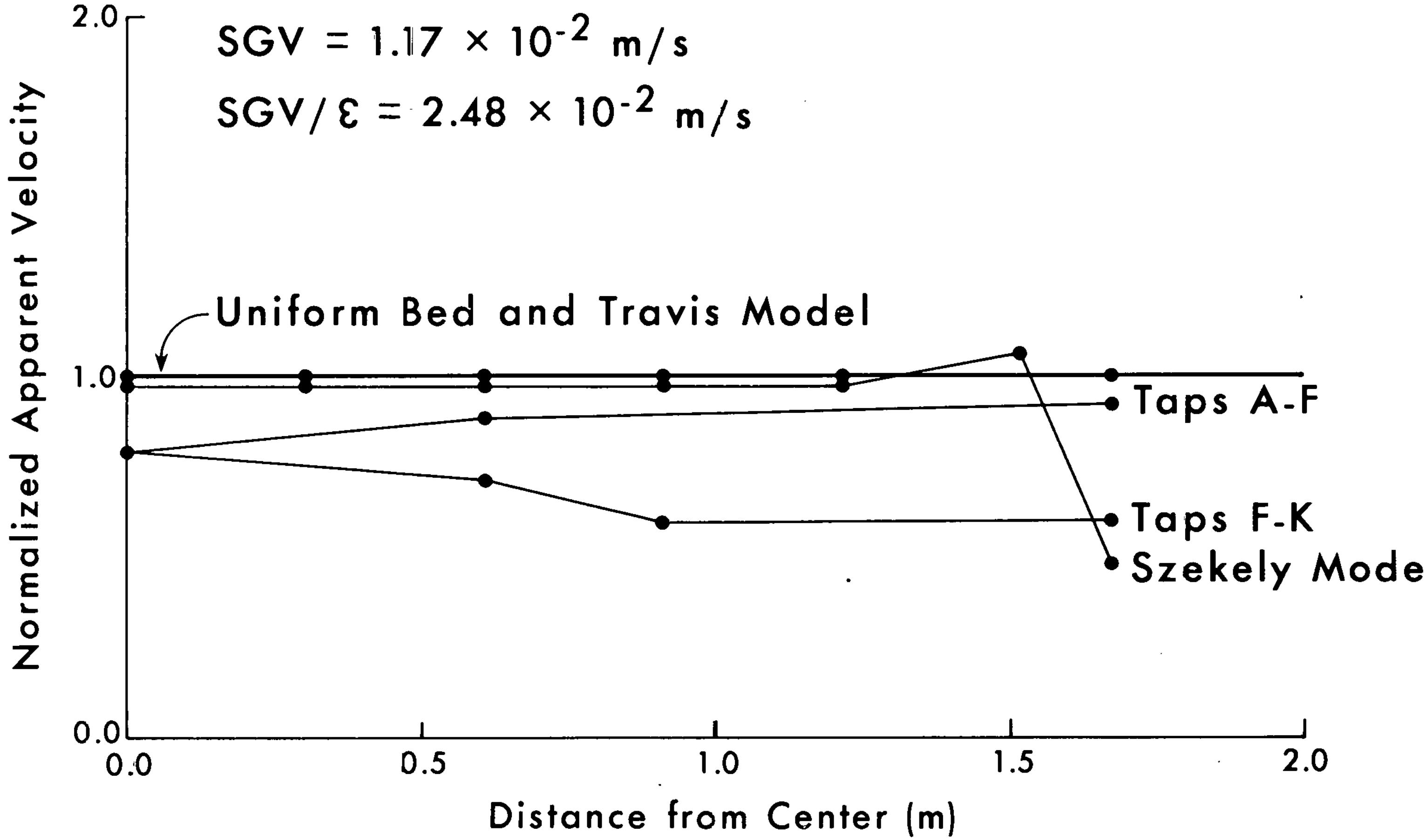

Figure 22. Level 2 to Level 3 Normalized Apparent Velocity, Stage 2

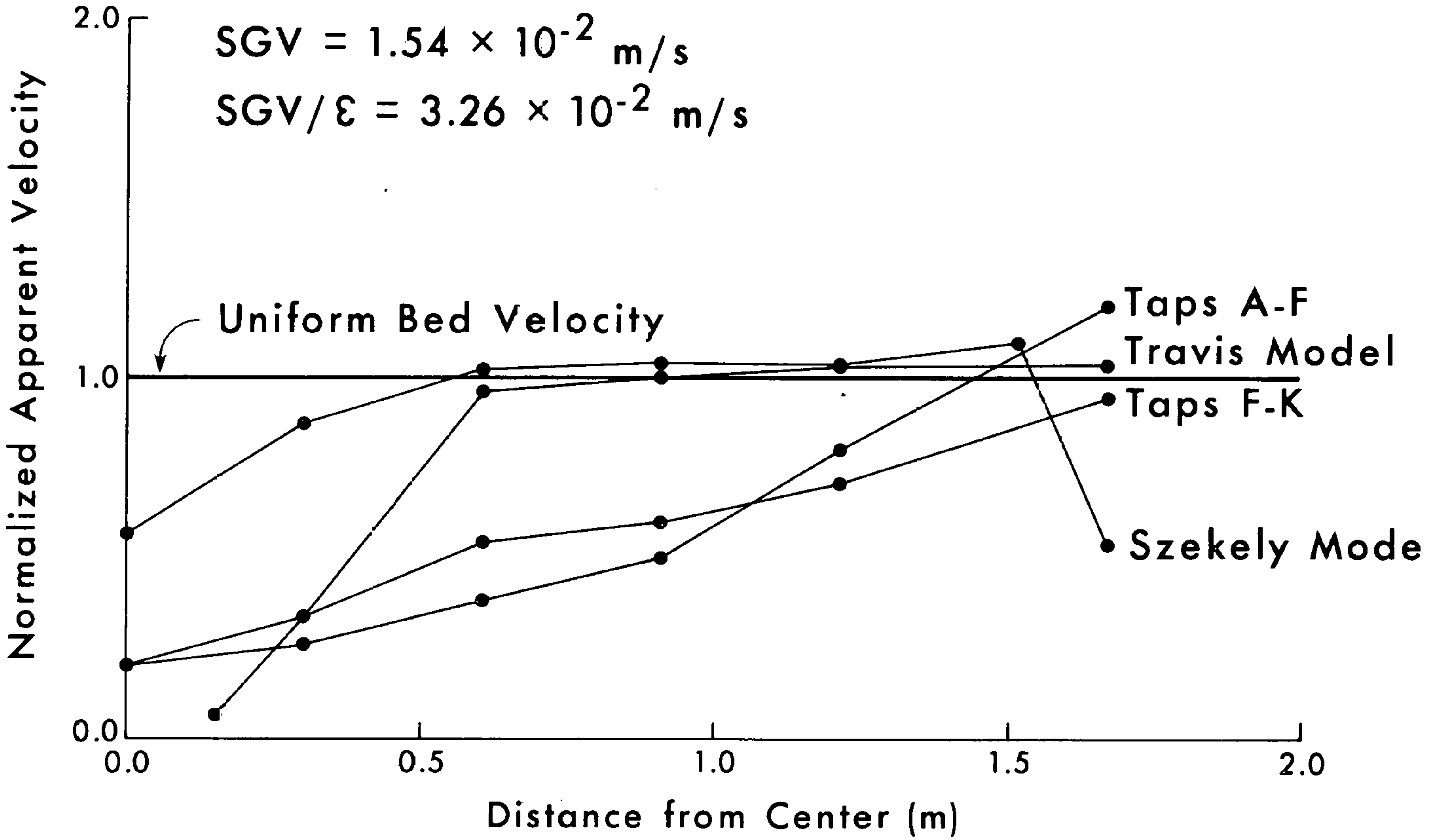

Figure 23. Level 1 to Level 2 Normalized Apparent Velocity, Stage 2

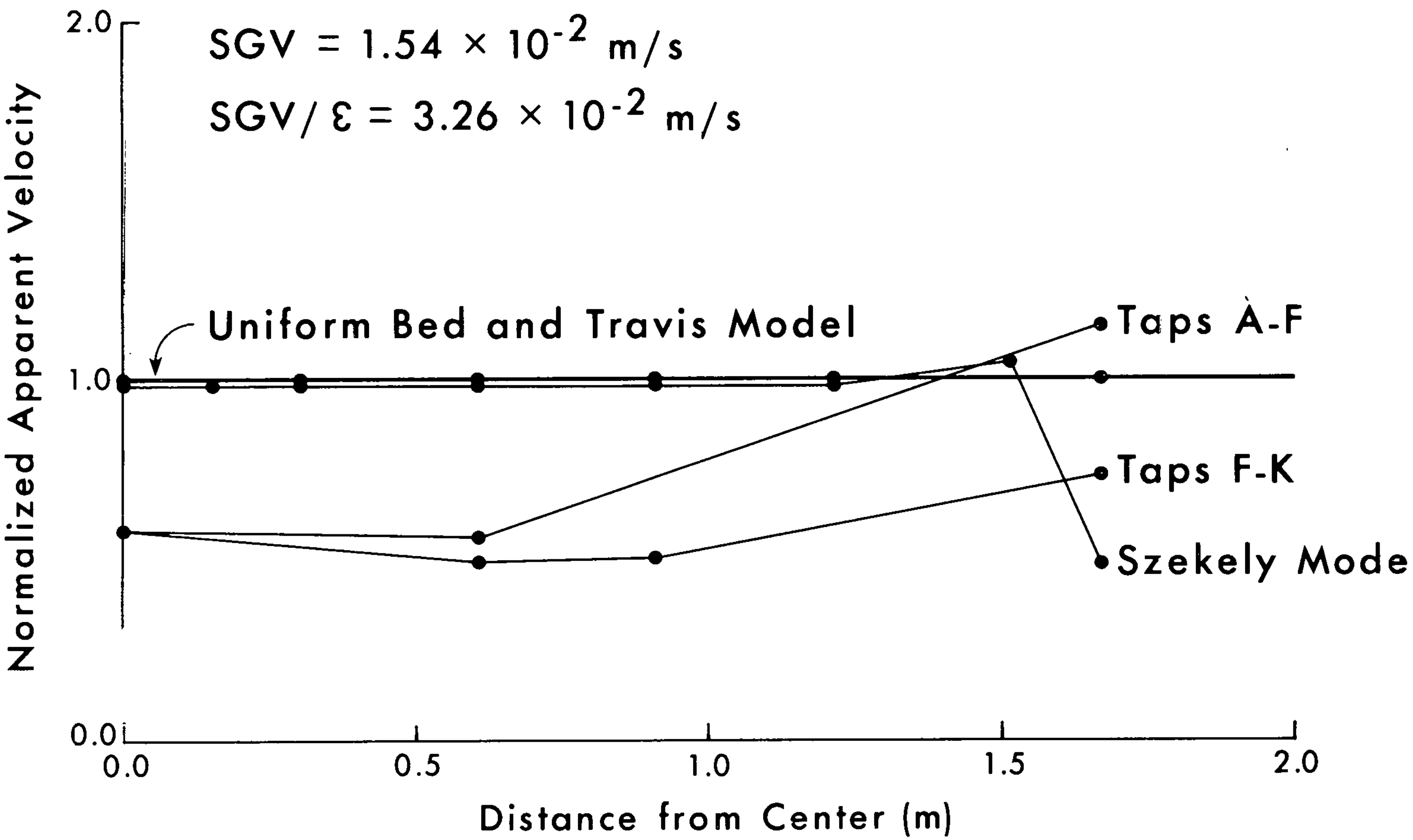

Figure 24. Level 2 to Level 3 Normalized Apparent Velocity, Stage 2

0.0117 m/s is shown in figure 25. This plot shows that the addition of the barrel increases the gas velocity near the center of the retort below the barrel while the velocities in stage 2 near the wall are less than or equal to the stage 1 velocities.

Steam Data

The thermal profiles from the steam flow test are shown in figures 26 through 37. The total time span of the test is 48 hours including the four hour hot airflow period. At probe levels 1 and 2 the shale near the north wall heats first, while at probe level 4 the shale near the south wall heat first. Temperatures toward the center of the retort tend to lag the outer temperatures. The level 2 temperature rise is the most uniform during the heatup period, followed by levels 3 and 4, with level 1 showing the least uniform rate of heatup.

Heat loss from the retort walls is shown in temperature profiles behind the steam front. Temperatures at the outside thermocouples level off 1 to 6 degrees Celsius below the second thermocouple in from the wall. Near the end of the test, when the entire bed is hot, the temperature decline at the outside thermocouple is greater at the south wall than at the north wall for all probe levels.

Figure 38 shows the temperature profiles at different times as the steam front moves down the retort. The 38°C profiles are plots of the temperatures on a given level the first time any thermocouple at that

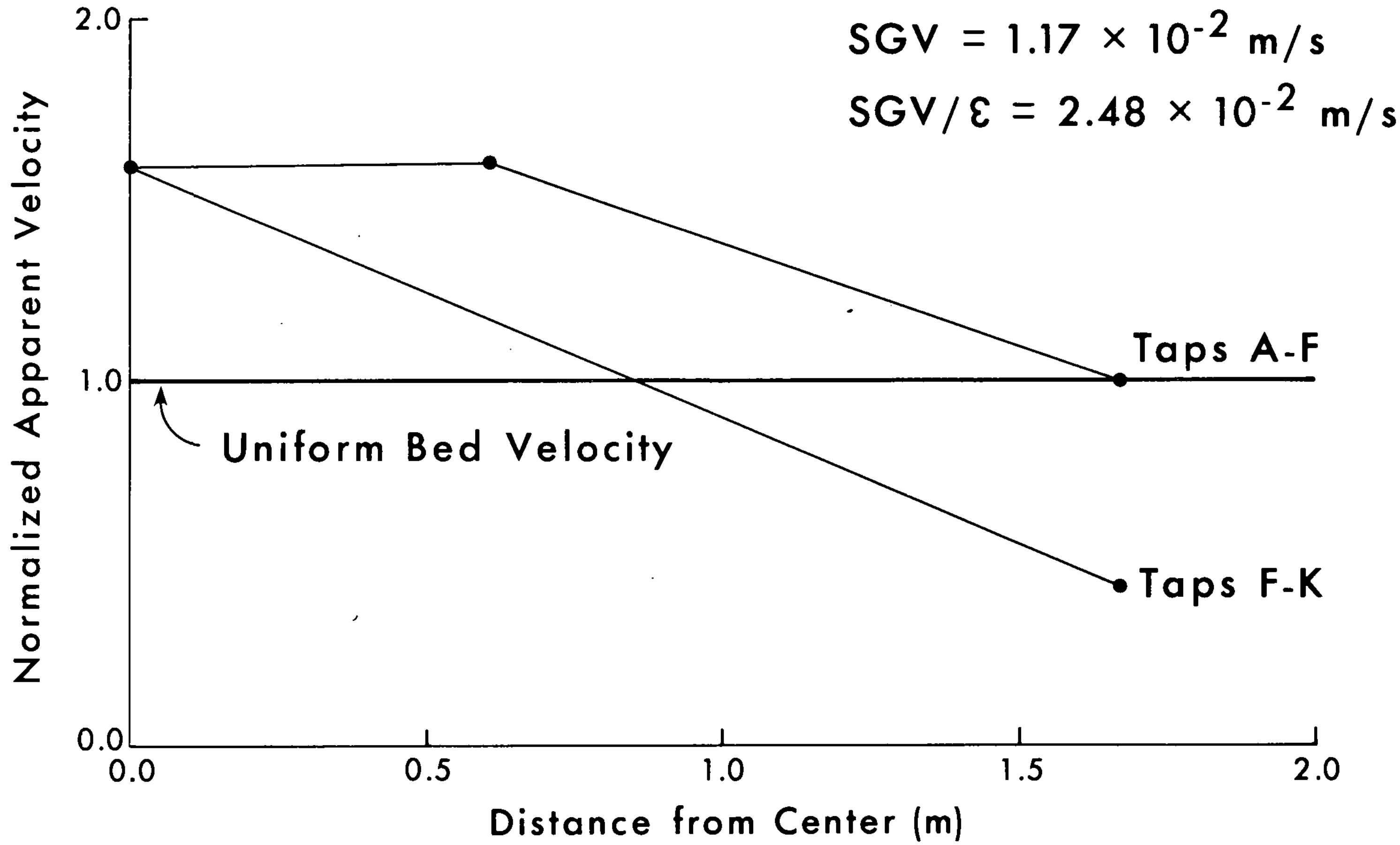

Figure 25. Level 2 to Level 3 Stage 2 Velocity Divided by Stage 1 Velocity

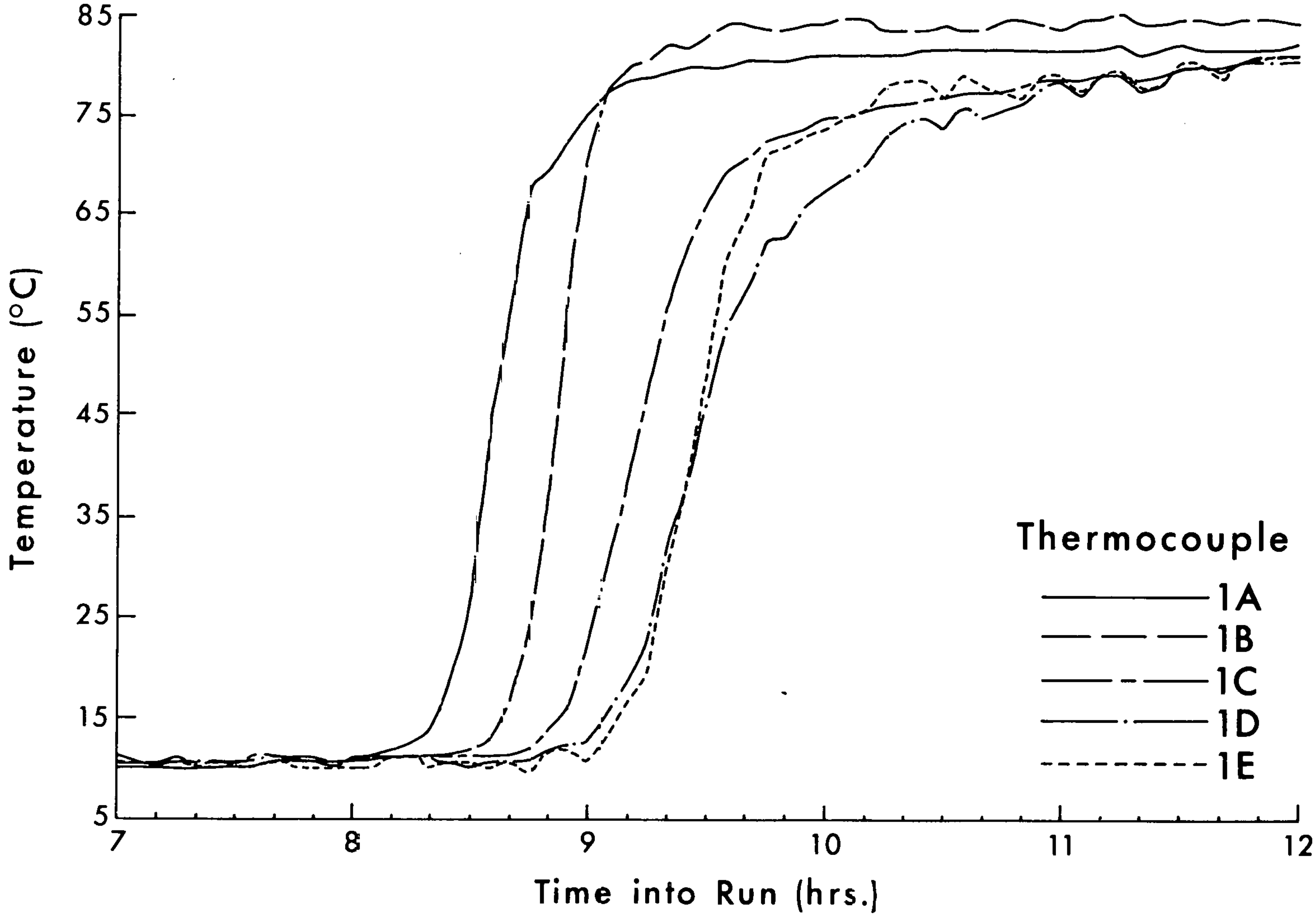

Figure 26. Steam Test Thermocouple Data

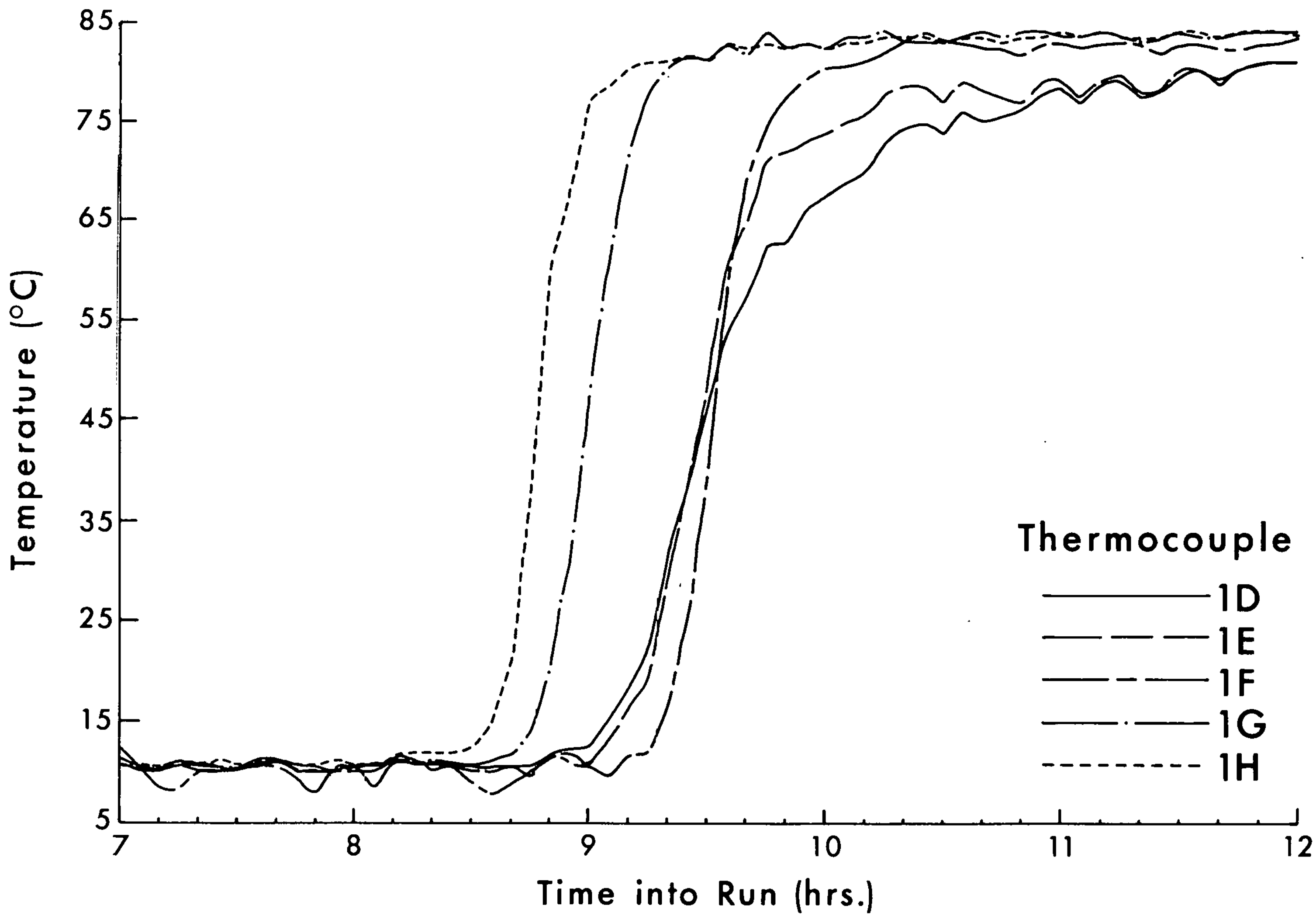

Figure 27. Steam Test Thermocouple Data

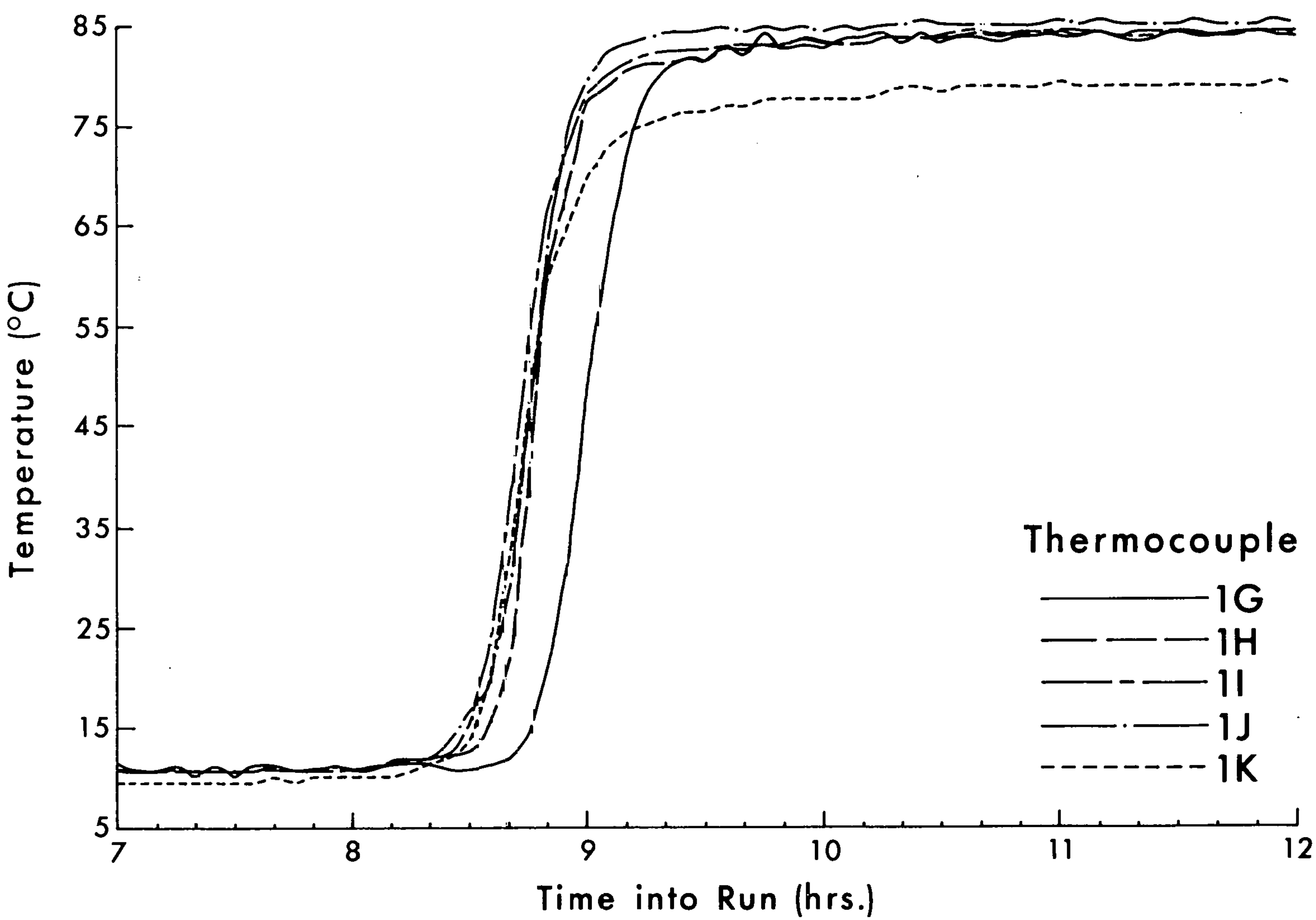

Figure 28. Steam Test Thermocouple Data

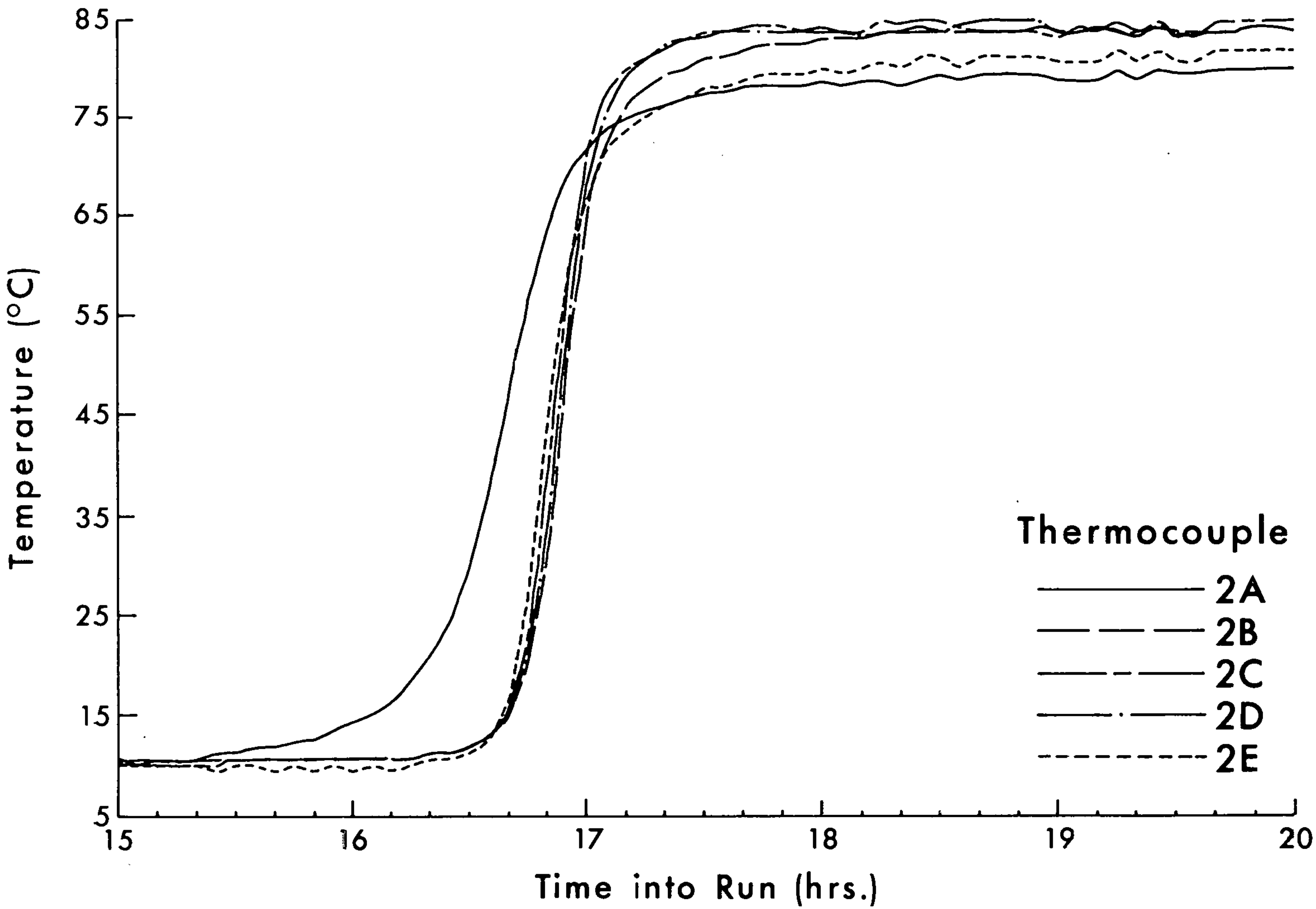

Figure 29. Steam Test Thermocouple Data

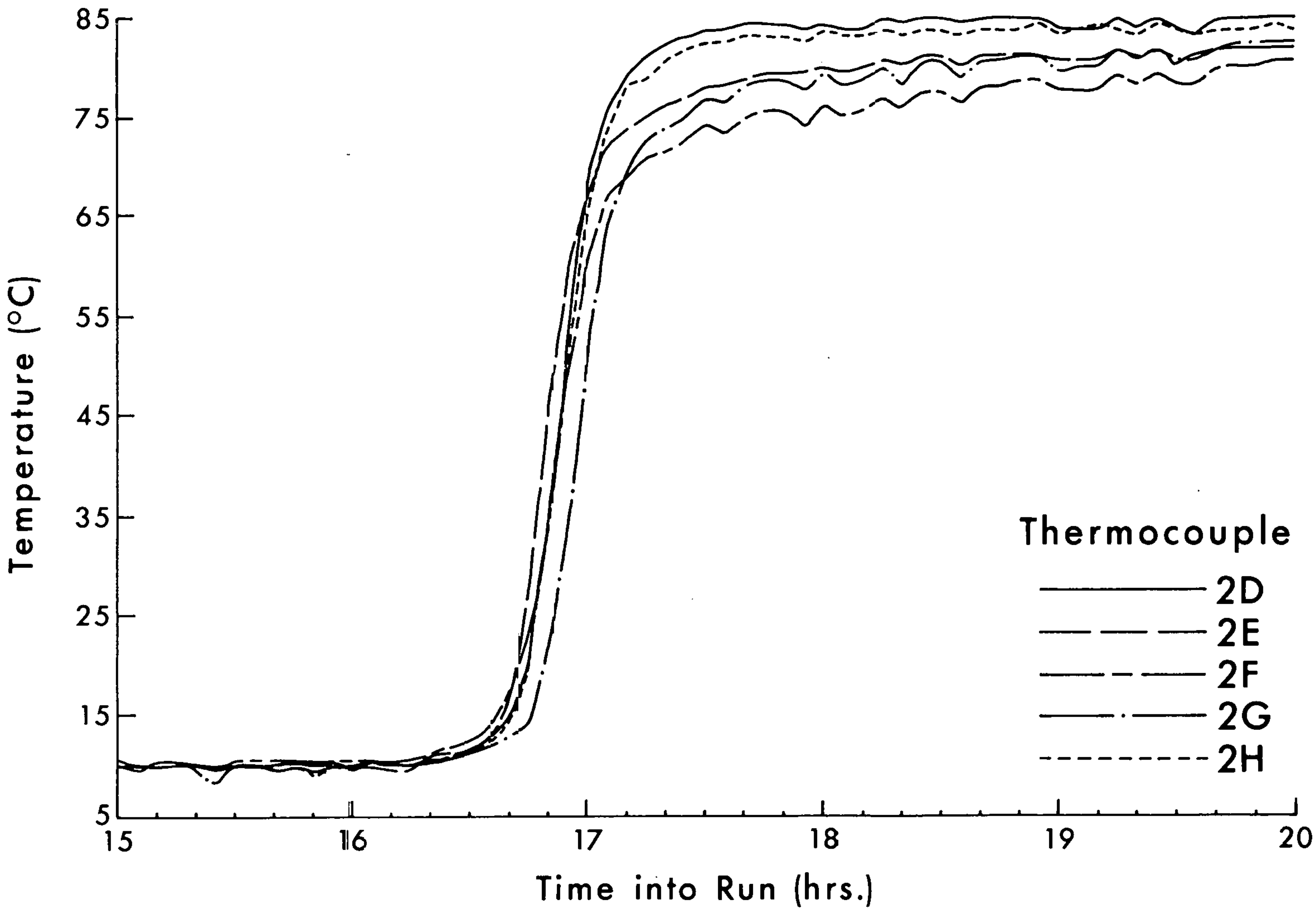

Figure 30. Steam Test Thermocouple Data

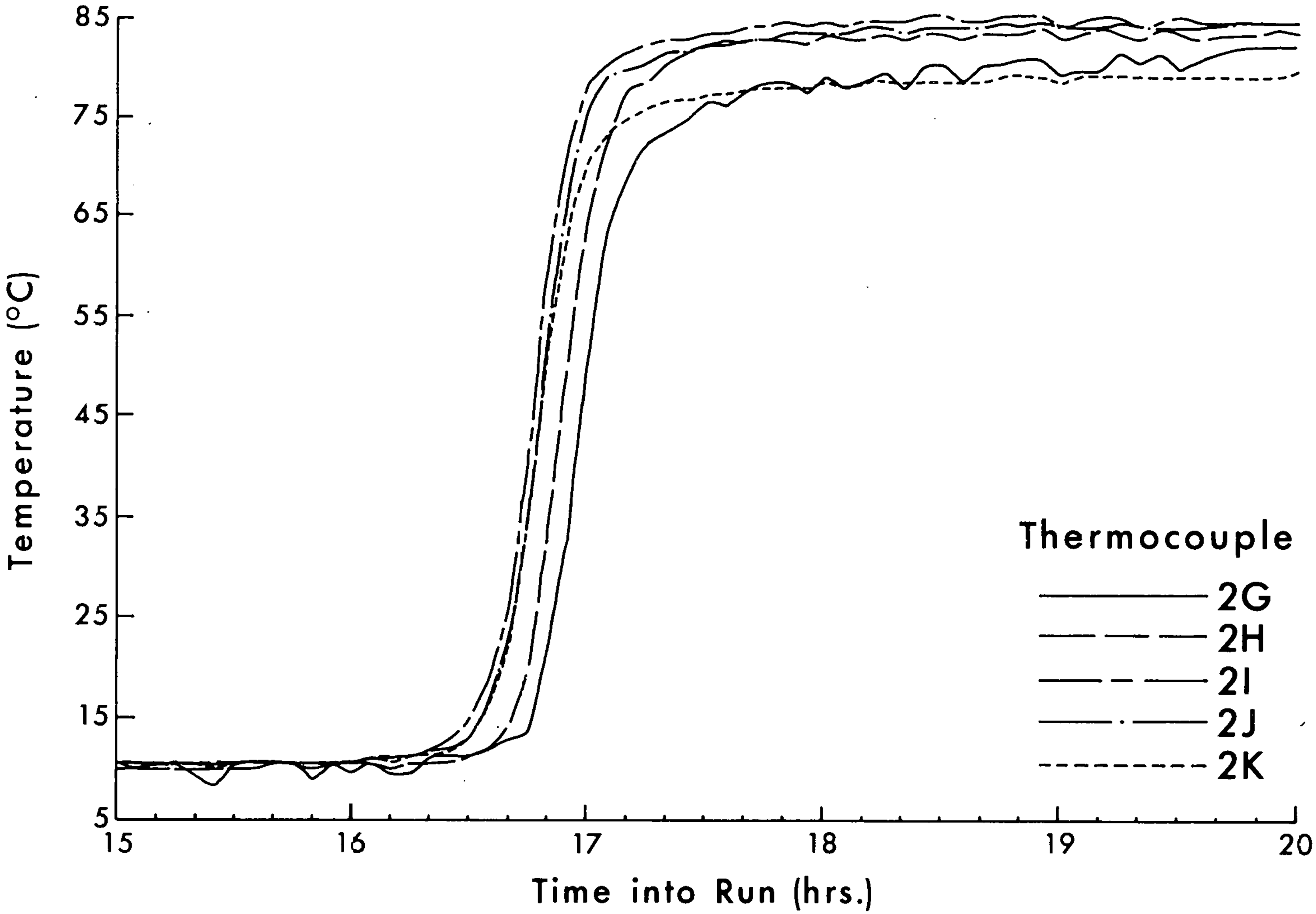

Figure 31. Steam Test Thermocouple Data

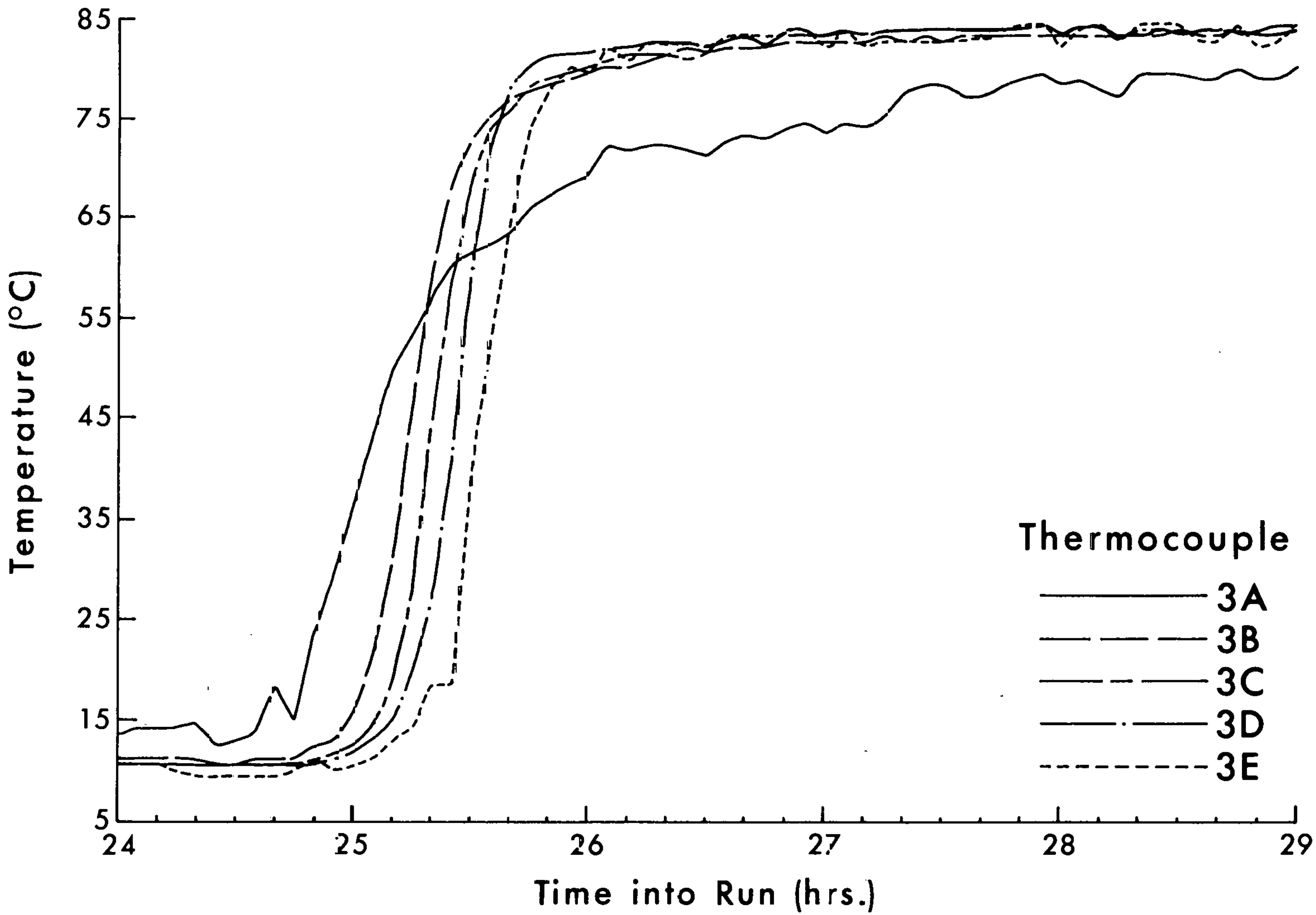

Figure 32. Steam Test Thermocouple Data

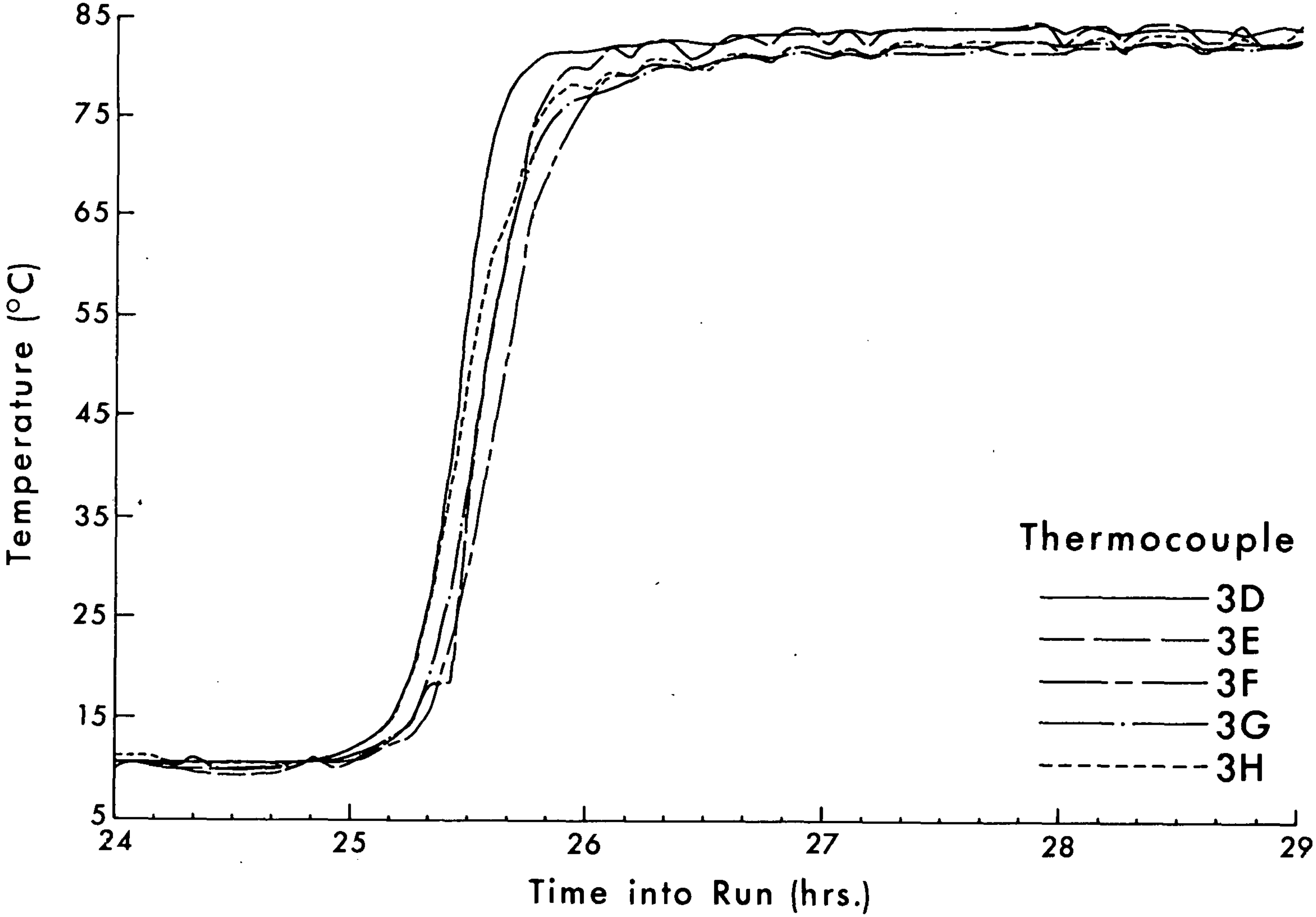

Figure 33. Steam Test Thermocouple Data

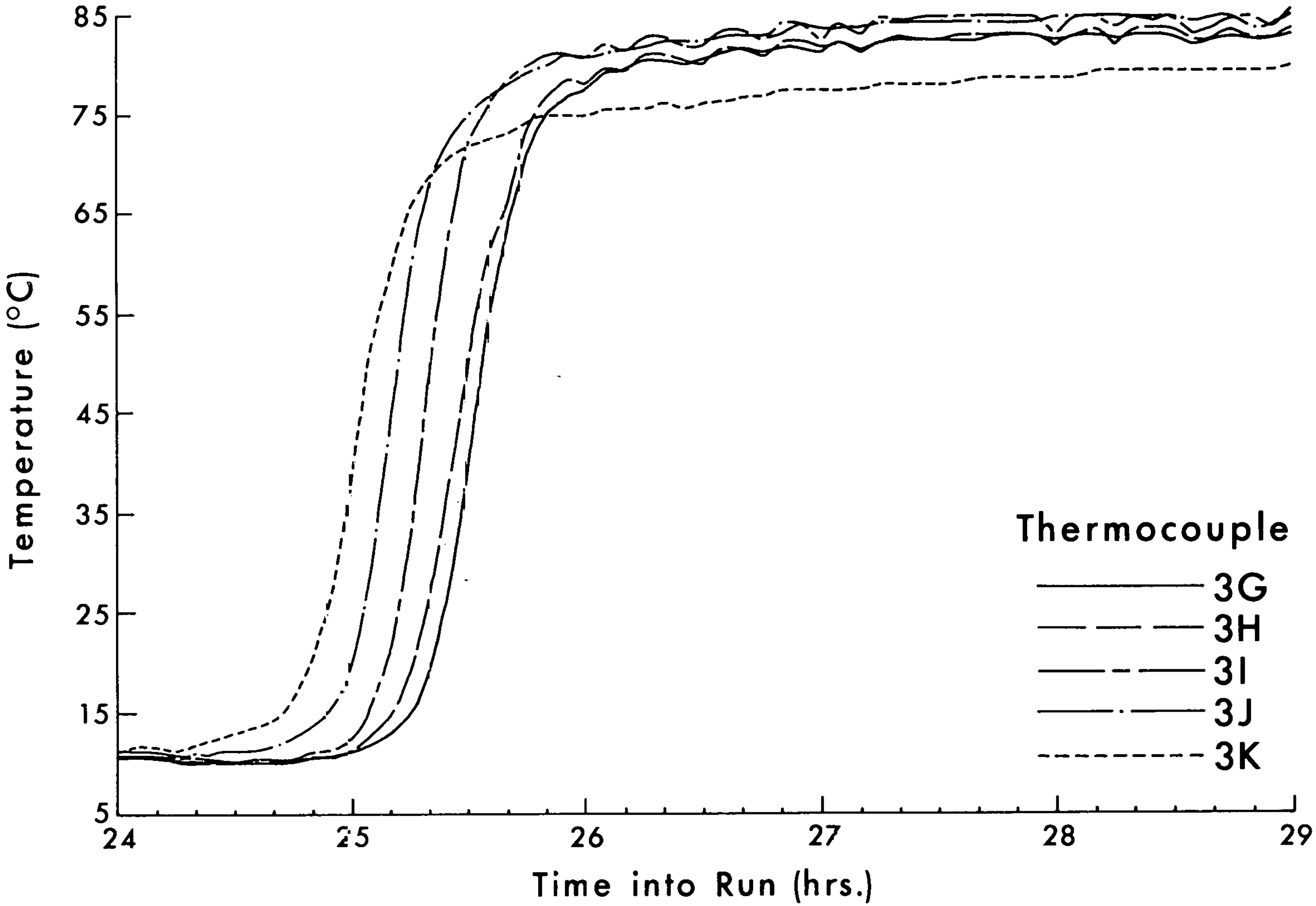

Figure 34. Steam Test Thermocouple Data

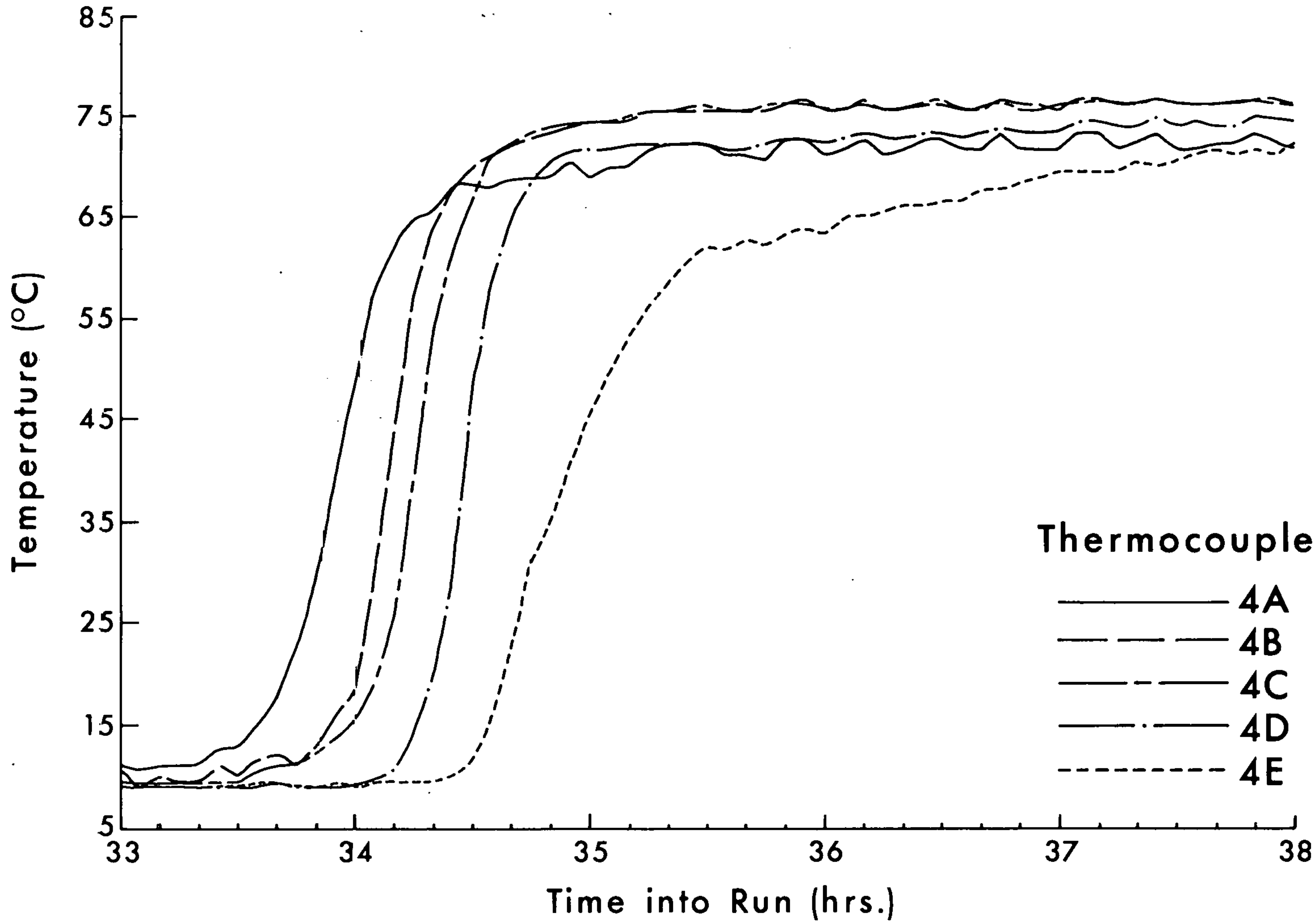

Figure 35. Steam Test Thermocouple Data

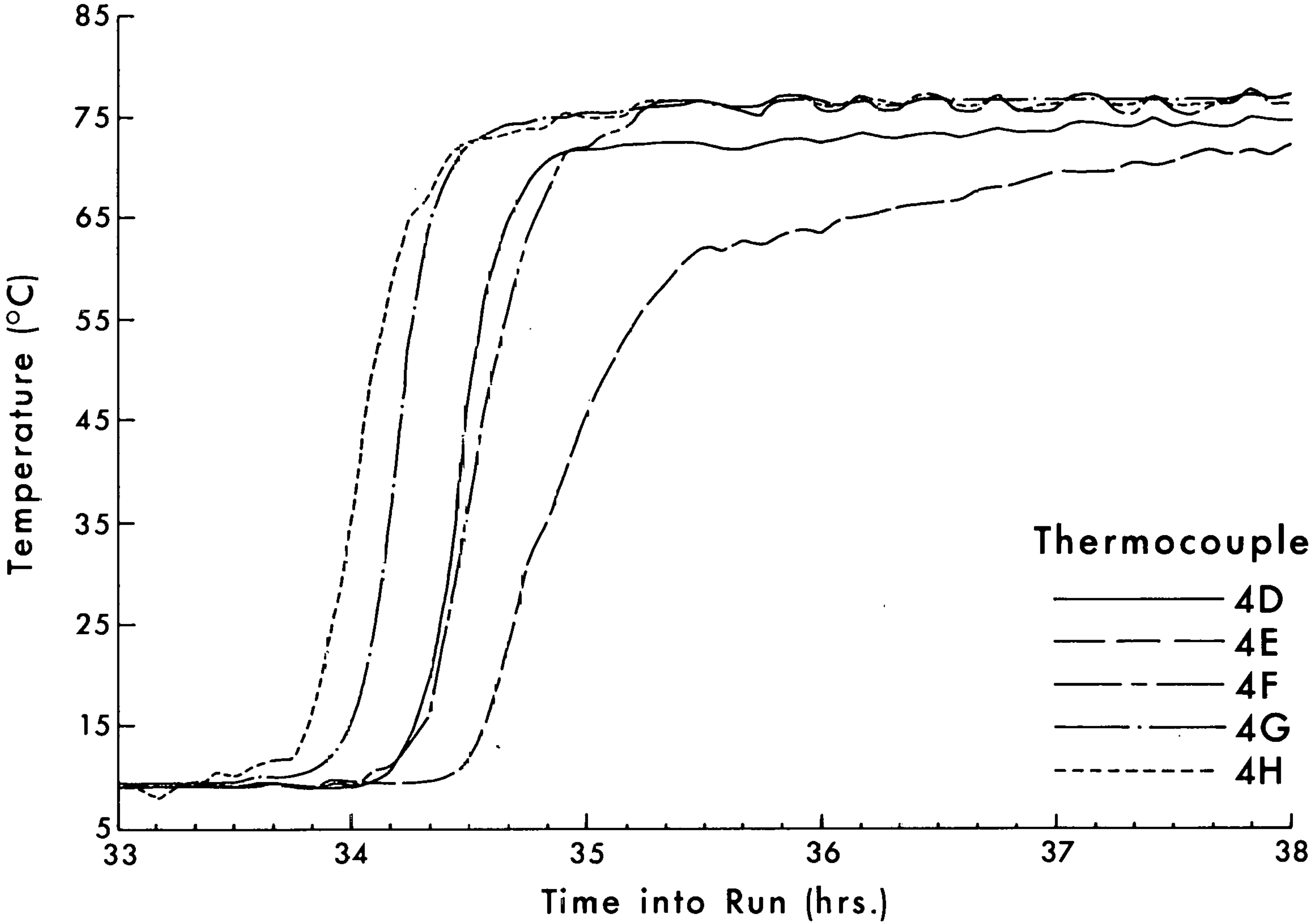

Figure 36. Steam Test Thermocouple Data

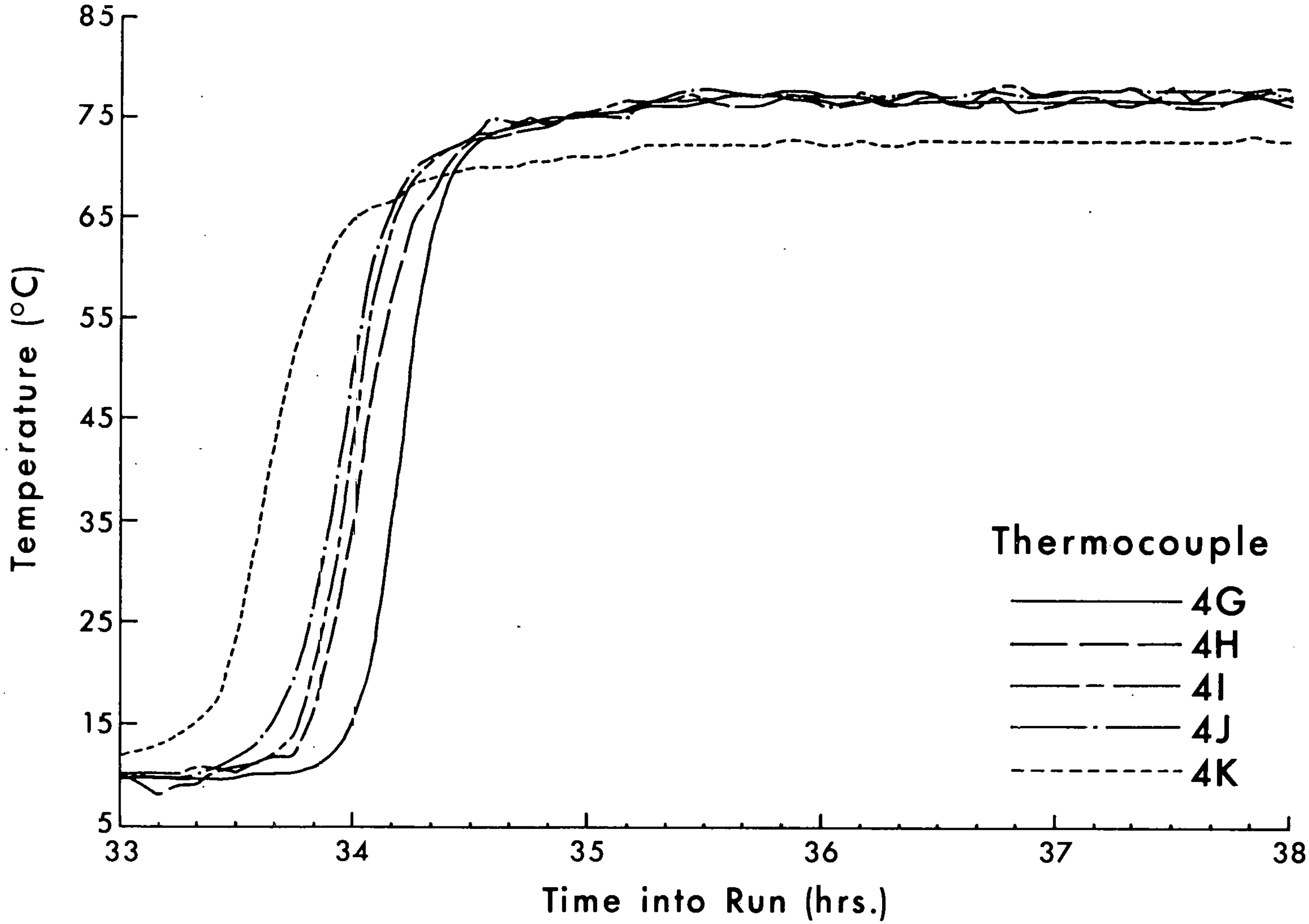

Figure 37. Steam Test Thermocouple Data

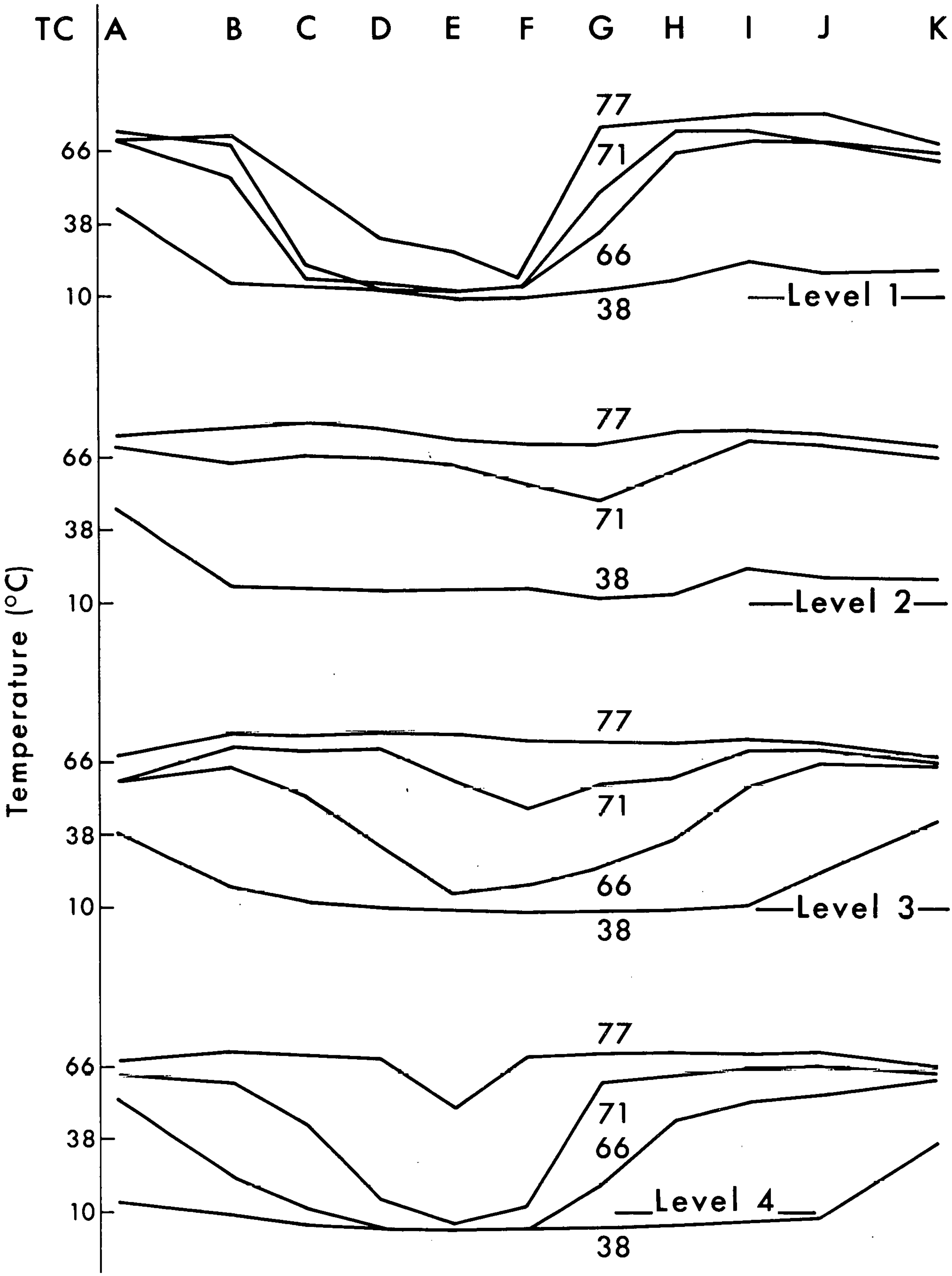

Figure 38. Steam Front

level reaches or exceeds 38°C. Similar criteria have been used to select data for the 66, 71, and 77°C profiles. Probe level 2 has only three profiles because the maximum temperature at that level goes from less than 67°C to more than 71°C in a single measurement period, resulting in identical profiles for the 67 and 71°C criteria.

The profiles at level 1 are consistant with a flow pattern that is not parallel to the long axis of the retort. The asymmetric flow may have been caused by fines in the shale bed or by end effects from flow entry into the top of the shale bed. The barrel being used as a flow obstruction may also contribute to the flow pattern at level 1.

Level 2 shows a uniform set of temperature profiles indicating a flow parallel to the long axis of the retort and uniform in velocity across the retort. Level 3 shows a lag in steam front approach near the center of the retort, which is probably due to a packing nonuniformity. Level 4 also shows a lag in the steam front approach, this time the lag is just left (north) of the center of the retort.

Figures 39 and 40 show the normalized steam front velocities between probe levels 1 and 2, and between 2 and 3, respectively. The velocities are normalized by the weighted average velocity at each level. In figure 39 the velocity near the centerline of the retort is higher than the velocity near the walls indicating that less energy is being used to heat shale in that region because the shale in the barrel is bypassed. Below the barrel, figure 40 shows that the steam velocities are nearly the same across the retort.

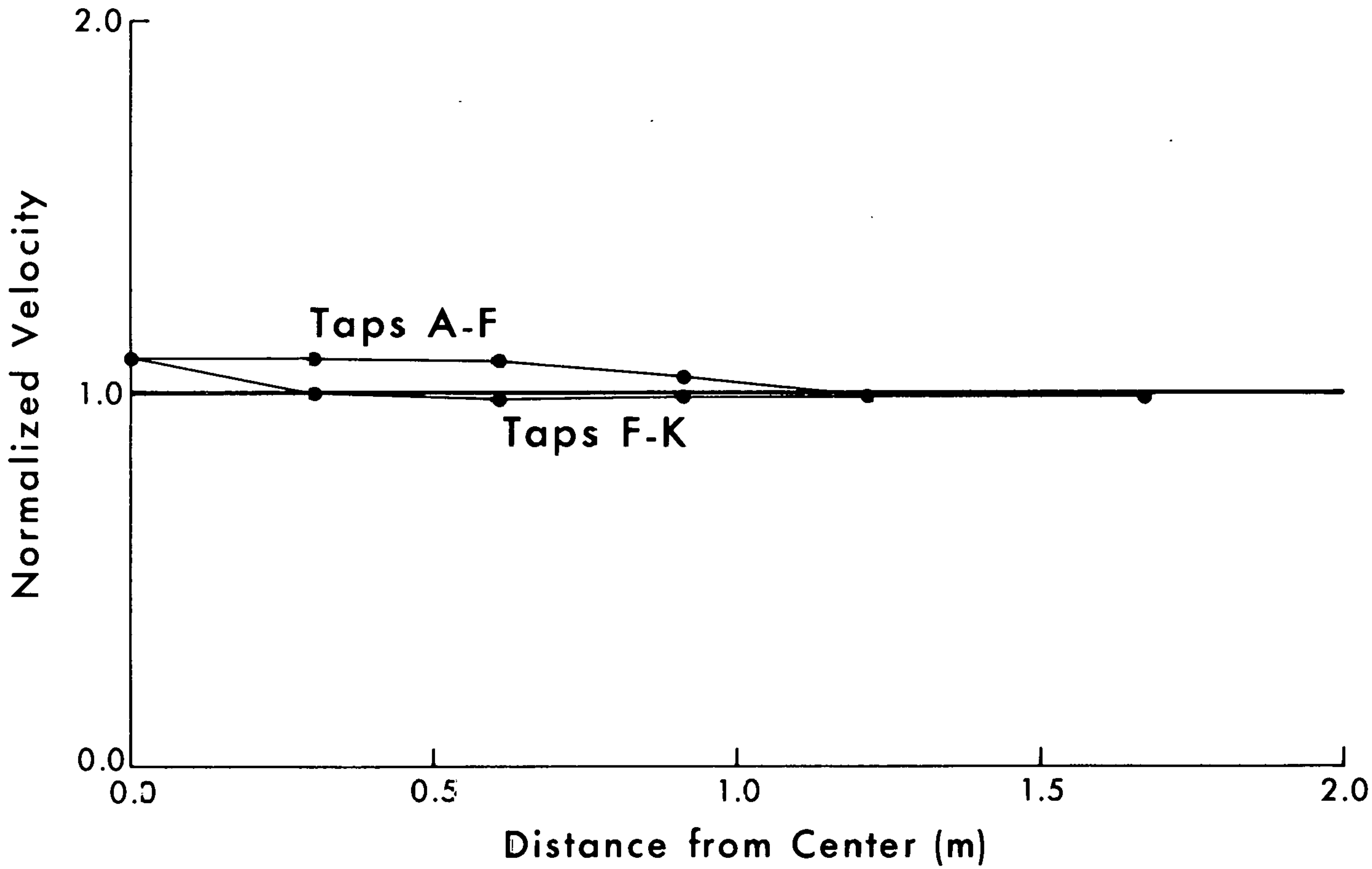

Figure 39. Level 1 to Level 2 Normalized Steam Front Velocity

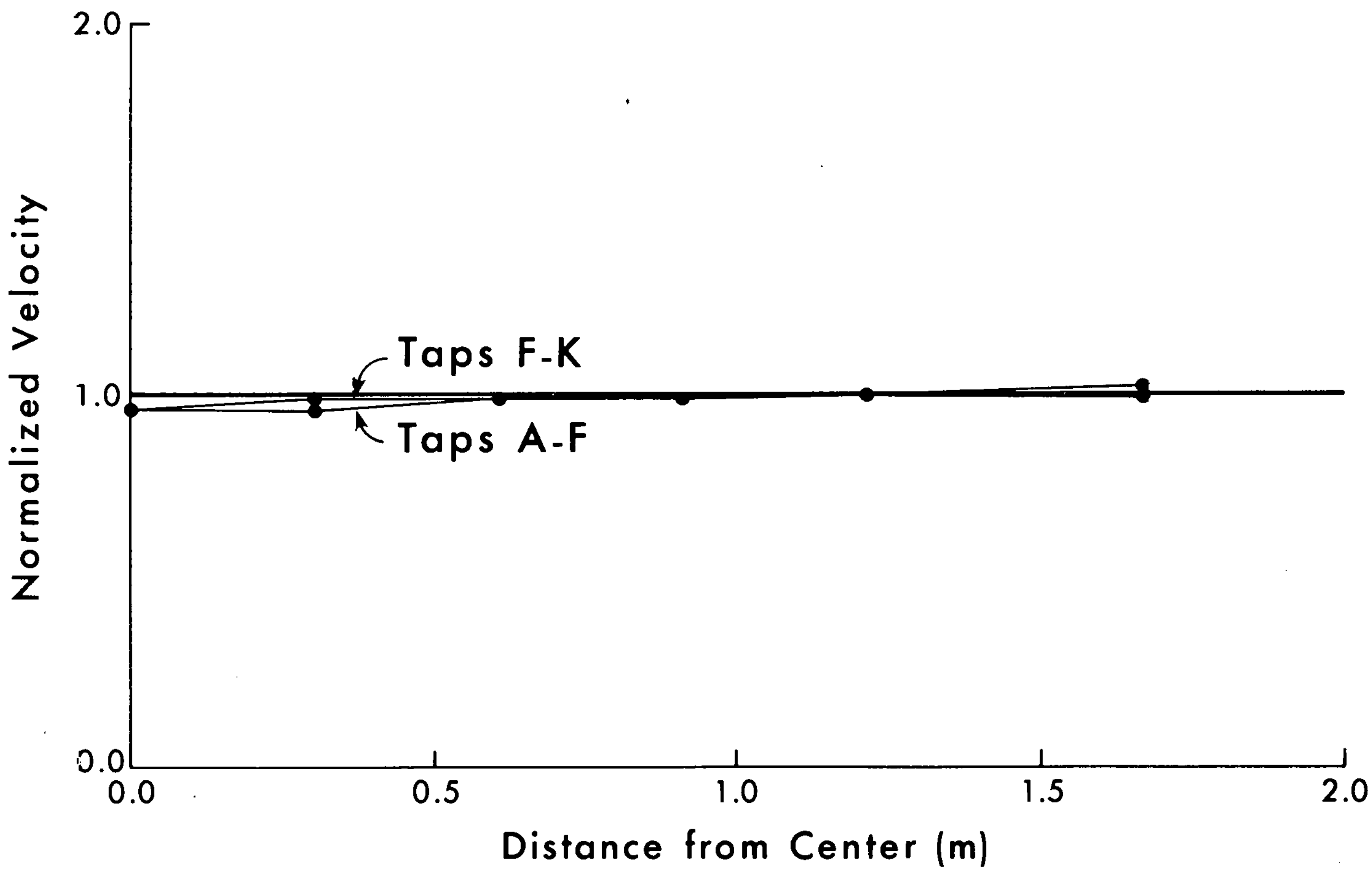

Figure 40. Level 2 to Level 3 Normalized Steam Front Velocity

Since it is not known to what extent the refractory is heated by the steam, the sweep efficiency of the steam front can not be accurately estimated. Depending upon the fraction of the refractory assumed to be heated, the calculated sweep efficiency ranges from 78% to 114%. The true sweep efficiency can not be greater than 100%.

CONCLUSIONS

The intent of this experiment has been to have a uniform rubble bed except for the barrel. Problems associated with screening and loading the shale have resulted in a nonuniform bed. This is evidenced by the radial variation in tracer velocities during the stage 1 tracer tests (figures 16-18). The velocities near the center of the retort are much lower than those near the walls. A uniform rubble bed should have no velocity variation except very near the walls. The steam test and the stage 2 tracer tests also show lower velocities below the barrel than near the walls although the effect is not as dramatic as with the stage 1 tracer tests.

The decrease in tracer velocities at the highest superficial gas velocity, as shown in figures 11 through 15, may be caused by either of two things. The first possibility is that at the higher flow rate much of the tracer is held in stagnant areas of the retort causing the tracer peaks to have anomolously long residence times. The second possibility is that the air flow measuring devices have lost calibration either during or just before the tests. The flow models do not predict this flow behavior.

The effect of the barrel on the steam front is small. There is some agreement between steam and tracer velocities between probe levels 2 and 3. Both sets of data show lower velocities in the center of the retort than at the walls. The tracer and steam tests between probe levels 1 and 2, however, do not show the same effect. The steam front perturbations were not sufficiently large to allow full characterization of the relationship between the tracer velocities and the steam front velocity.

It has been shown by the sensitivity analysis that small rubble bed nonuniformities cause measurable flow perturbations. Furthermore, the tracer test results indicate the presence of nonuniformities that are not observed in the steam test results. This demonstrates that the tracer method has superior resolution to the steam front method for rubble bed characterization, however, the method has certain problems which should be addressed.

RECOMMENDATIONS

In order to solve some of the problems described in this report several areas need further study. A larger obstruction is needed to cause a greater perturbation of the steam front shape. This would allow a more comprehensive comparison of steam data with tracer data to be made. As part of this study the retort should be better instrumented to determine heat losses so that an accurate steam front sweep efficiency can be calculated.

In conjunction with WRI's tracer testing program on the large retorts a large number of small scale tests are needed to determine several basic relationships. This report shows one instance where repeated injections at the same tap do not always produce the same response curve. A study needs to be made to determine the relationship of tracer response curve shapes to injection variables such as injection point geometry, injection pressure and injection volume.

The flow perturbation "shadow" caused by the barrel in this report was not very large. The effect of obstruction size and the distance of the obstruction from the injection and detection taps needs to be studied. The results of such a study may allow researchers to determine whether a tracer test can resolve the difference between a small obstruction near the injection point and a larger obstruction farther away.

Several examples of multiple peaks are shown in this report. Techniques of separating and characterizing the multiple pathways indicated by these peaks must be developed. Signal processing methods may be of use in determining the exact spacing of overlapping peaks.

REFERENCES

1.) R. A. Loucks, "Occidental Vertical Modified In Situ Process for the Recovery of Oil From Oil Shale: Phase I Final Report for the Period November 1, 1976 through April 30, 1979", Occidental Oil Shale, Inc., G. J. Co., 1979.

2.) T. C. Bickel, "Analysis of Occidental Vertical Modified In Situ Retorts 7 and 8", 16th Oil Shale Symposium Proceedings, Colorado School of Mines Press, p. 281, 1983.

3.) K. L. Berry, R. L. Hutson, J. S. Sterrett, and J. C. Knepper, "Modified In Situ Retorting Results of Two Field Retorts", 15th Oil Shale Symposium Proceedings, Colorado School of Mines Press, p. 385, 1982.

4.) M. L. Gregg and J. H. Cambell, "Sweep Efficiency Modeling of Modified In Situ Retorts", 13th Oil Shale Symposium Proceedings, Colorado School of Mines Press, p. 87, 1980.

5.) A. E. Harak, L. Dockter, A. Long and H. W. Sohns, "Oil Shale Retorting in a 150-Ton Batch-Type Pilot Plant", RI 7995, U. S. Department of Interior, 1974.

6.) B. J. Travis and T. L. Cook, "Numerical Simulation of Fluid Flow in Porous/Fractured Media", 5th AIME Uranium Seminar, 1981, Albuquerque, New Mexico.

7.) C. A. Romero and J. E. Uhl, "Characterization of a Non-Uniform Retort Using Tracer Techniques", Summer National AIChE Meeting, 1983, Denver, Colorado.

8.) J. Bear, Dynamics of Fluids in Porous Media, American Elsevier Publishing Company, Inc., New York, 1972.

9.) S. Ergun, "Fluid Flow Through Packed Columns", Chemical Engineering Progress, v. 48, no. 2, 1952, pp. 89-94.

10.) R. A. Minster and D. W. Fausett, "Fluid Flow Through Packed Columns of Crushed Oil Shale, Report of Investigation, U. S. Department of Energy, Laramie Energy Technology Center, Number LETC/RI-80/5, Distribution Category UC-91.

11.) V. Stanek and J. Szekely, "Three Dimensional Flow of Fluids Through Nonuniform Packed Beds", AIChE Journal, vol. 20, No. 5, p. 974, 1974.

12.) J. Szekely and J. L. Poveromo, "Flow Maldistribution in Packed Beds: A Comparison of Measurements with Predictions", AIChE Journal, vol. 21, No. 4, p. 769, 1975.

13.) J. Szekely and M. A. Propster, "The Structure and Flow Resistance of Layer Charged Particulate Systems in the Modeling of Gas Flow through Simulated Blast Furnace Burdens", Transactions of the Iron and Steel Institute of Japan, vol. 19, No. 1, 1979.

14.) M. A. Propster, "Gas Flow Phenomena in the Stack Region of the Ironmaking Blast Furnace", Doctoral Thesis, State University of New York, 1977.